Hurricane Ophelia: A case study of dynamically downscaled model analysis under alternate climate scenarios

Marjolein Ribberink

Supervisors:

Dr. Hylke de Vries
Dr. Nadia Bloemendaal
Dr. Michiel Baatsen

A thesis presented for the degree of
Master of Science

Institute for Marine and Atmospheric research Utrecht (IMAU)
Utrecht University
Netherlands
February 23, 2024

Abstract

Tropical cyclones are both deadly and costly disasters, though their impact on Europe is infrequently studied due to relatively few occurrences. However, recent studies suggest the number and impact of tropical-origin storms affecting Europe is likely to increase with future warming.

We present a case study of one recent Europe-impacting storm, 2017's Hurricane Ophelia, examining its representation in analysis datasets (ERA5, GFS, and the ECMWF Operational) as well as in simulations of these datasets downscaled with the regional model RACMO. The ECMWF-based models do not accurately simulate Ophelia, especially in the tropical phase where Ophelia's central pressure is overestimated by more than 30 hPa.

Applying a uniform temperature forcing ranging between -2 to +4 °C to the GFS-driven RACMO simulations allows us to model alternative climates. In warmer climates the storm grows larger and stronger than in the present-day scenario, moving faster and further from land. Despite this, the wind speeds experienced on the Irish Coast are higher than when it impacts the coast directly in the present-day scenarios. Additionally, its extratropical transition proceeds differently: in the warmest scenarios Ophelia does not complete extratropical transition, but continues to resemble a warm-core tropical cyclone.

Acknowledgements

This thesis, while a genuine pleasure to complete, could not have come together without the support of several very key people.

First and foremost, I have to thank my supervisors at KNMI, Dr. Hylke de Vries and Dr. Nadia Bloemendaal, without whom this would not have come together as it has. They were always available to answer my questions, made me think further than the face-value answers, and reminded me to also take a break! I would also like to thank Dr. Michiel Baatsen as my supervisor at Utrecht University, who always had a new idea to expand my research and make it more rigorous, expanding my knowledge of this subject. I want to extend my thanks also to Erik van Meijgaard, who set up and ran the RACMO simulations for this research project, for which I am very grateful.

To all the other people who walked with me throughout this: you made this project possible by enouraging me to keep going when it was tough and offering distractions when necessary. You are very appreciated and I could not have accomplished this without you!

Contents

1 Introduction

Tropical cyclones (TCs) are some of the most dangerous and destructive phenomena on the planet. In the last 10 years, more than 650 billion dollars (2023 adjusted) in damages were done by TCs in the United States alone (Smith, 2023). These numbers are only expected to increase without mitigation: climate change is projected to bring more intense storms and the populations in at-risk areas are growing in size and wealth (Knutson et al., 2010; Mendelsohn et al., 2012; Pielke et al., 2008). We have seen some effects of this already: of the 15 costliest TCs to impact the United States, only 1 occurred outside the last 20 years (Smith, 2023).

Another facet of the increasing damage costs moving into the rest of the century and beyond is the shifting and expanding of the at-risk area. Several studies have shown that the average storm track latitude has been tracking poleward (Daloz and Camargo, 2018; Kossin et al., 2014; Studholme et al., 2022). Western Europe is also likely to see an increase of TCs and post-tropical cyclones (PTCs), as warming sea surface temperatures (SSTs) expand the cyclone genesis and occurrence regions (Baatsen et al., 2015, hereafter B2015; Dekker et al., 2018; Haarsma et al., 2013; Liu et al., 2017).

Many of these Europe-impacting TCs experience interaction with the mid-latitude atmosphere and lose their tropical nature, taking on characteristics of extratropical cyclones (ETC) (S. C. Jones et al., 2003). This so-called extratropical transition (ET) changes the structure of the storm, which grows asymmetric, starts tilting with height, and develops frontal structures resembling those of ETCs (Hart, 2003; S. C. Jones et al., 2003; Thorncroft and Jones, 2000). Hart and Evans (2001) found that nearly half of all North Atlantic TCs undergo ET at some point in their lifetime.

B2015 describe a hypothetical case that appeared in their simulations of warmer climatic conditions whose characteristics and lifecycle replicated many of the features seen in storms that make landfall in Europe. This case, which they called Amy, is a TC that transitions to a warm-core ETC as it interacts with an upper-level trough in the midlatitudes, at which time it intensifies before impacting Western Europe.

Amy has a stunningly similar real life equivalent in 2017's Hurricane Ophelia. Appearing a mere two years after B2015 described Amy, its peculiar lifespan started as a small but strong TC. Ophelia developed winds of 185 km/h, which equates to Category 3 on the Saffir-Simpson scale (Simpson and Saffir, 1974; Stewart, 2018). Hurricanes of Category 3 and higher are considered major hurricanes, and Ophelia was the easternmost major hurricane to form in the North Atlantic since the satellite era (see Figure 1). Just like Amy, Ophelia interacted with a midlatitude trough that sent it rocketing towards Europe as it underwent ET and reintensification (Stewart, 2018).

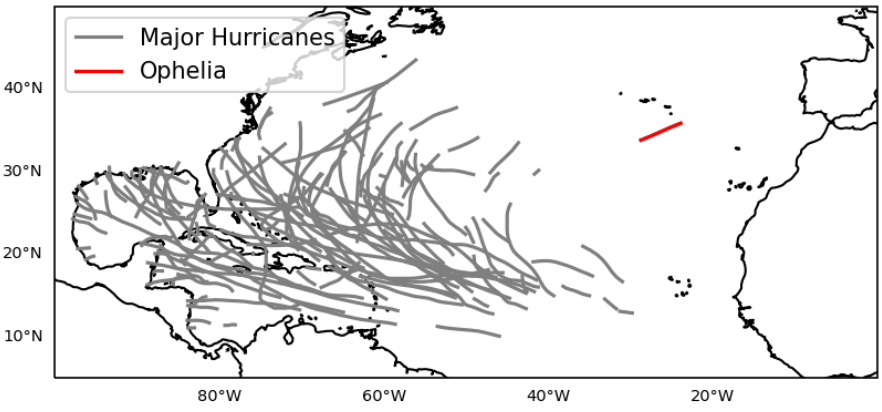

Figure 1: All North Atlantic major hurricane tracks 1979-2022, with Ophelia's track while a major hurricane highlighted in red.

Ophelia made landfall in Ireland on 16 October 2017 as a PTC, with 10-minute sustained winds of over 100 km/h, and brought the highest wind gust ever recorded in Ireland at 191 km/h (NDFEM, 2019). These high winds led to hundreds of downed trees, causing the storm's three fatalities and isolating outlying communities. The early fall timing of this storm meant more trees were in full leaf than during the typical winter storm season, consequently the impact was likely greater than it would have been had it occurred later in the year (Met Éireann, 2018). With

hurricane season spanning June-November, this impact is one we can expect to see repeated with more Europe-impacting TCs and PTCs.

Ophelia also caused substantial damage to the Irish electricity network, leaving more than 385,000 premises without electricity, some of which were not restored for a week. Additionally, on its way north, Ophelia's strong outflow winds fanned wildfires in Portugal that caused 51 deaths and burned more than 200,000 ha of land (Met Éireann, 2018; San-Miguel-Ayanz et al., 2020).

Rantanen et al. (2020) studied Ophelia's ET, discovering that Ophelia's environment met several conditions described by Hart (2006) as indicators for post-ET strengthening. They also note that the ECMWF OpenIFS model they used was unable to adequately simulate the central pressure of the tropical phase of the storm (before Ophelia started ET).

Despite all the improvements made over the last few decades, modelling TCs continues to be a challenge (Camargo and Wing, 2016). Large-scale global models (and their analysis datasets) are able to simulate the necessary long timescales and large spatial extent, but even the very high resolution and thus expensive models are inadequate to accurately simulate the structure of especially strong storms, such as TCs, often leading to intensity underestimation (Davis, 2018). Regional models are capable of getting to much finer resolutions, but their spatial and temporal extent are much more limited due to their associated costs. Additionally, regional models are often 'uncoupled' models: atmosphere-only models without a connected ocean model. Instead, uncoupled models simulate the ocean with heat fluxes or a simple prescribed SST. This does reduce computation costs, but oversimplifies the complicated ocean-atmosphere interaction. Unlike ETCs, TCs draw their energy straight from the warm ocean water underneath them, which entails a stronger ocean-atmosphere connection. Several studies have shown that coupled models outperform the uncoupled versions of the model when simulating TCs (Ito et al., 2015; Srinivas et al., 2016).

One solution to this is to use coarser datasets as the initial and boundary conditions to run a regional model, a process known as dynamical downscaling. The boundary conditions continue to input data from the coarser datasets into the finer regional model, allowing a finer resolution in the area of interest and the information from outside it without the prohibitive costs of running the regional model over the whole domain. However, it does come with a downside: these regional models are sensitive to the conditions and biases already present in the global model (Xu and Yang, 2012). One such regional model is RACMO (**R**egional **A**tmosphere **C**ommunity **MO**del). It has been used with success for this purpose, for example by Dullaart et al. (in press) to downscale TCs in the Caribbean region. They downscaled reanalysis data and showed that RACMO can be used to derive a climate change signal in TCs using a simple applied ΔT approach.

In this study, we examine Hurricane Ophelia simulated in RACMO, initialized by global analysis datasets. This is done in order to explore two main research directions. First, we want to explore how well Ophelia is captured in analysis datasets. These are some of the most commonly used datasets in the scientific community as they are freely available, have good coverage temporally and spatially, and contain many different variables. Knowing how Ophelia is simulated in these datasets is important as an indicator of how well future, higher-impact storms may be simulated by such datasets. Second, we want to know how Ophelia behaves in other climate scenarios. As Ophelia is a representation of what we may expect more often with future warming, being able to determine the changes this future warming may impart to such a storm is important to minimize future damages and loss of life.

Our case study is described in more detail in Section 2. Descriptions of our data, models, cyclone tracking methods, ET quantification, and impact determination can be found in Section 3. The main results and accompanying discussions are presented in Section 4, examining Ophelia's behaviour in different datasets, with different initialization times, and under alternate climate conditions. Section 5 examines our limitations and identifies areas of future research. The paper is concluded in Section 6.

2 Case Study Description

Hurricane Ophelia was not the strongest or most destructive hurricane of the 2017 Atlantic season, but it was one of the most remarkable due to its interaction with Europe. It is also the furthest east major Atlantic hurricane recorded since satellite observations started in 1979 (Stewart, 2018); Figure 1 shows the tracks of all major Atlantic hurricanes in that time period, with Ophelia in red. At its strongest, Ophelia was a Category 3 with sustained 10-minute wind speeds of 172 km/h, with a minimum central pressure of 957 hPa (Stewart, 2018). It hit Ireland at 11Z on October 16

as a PTC with peak sustained (10-minute average) winds of 145 km/h and gusts to 191 km/h.

Hurricane Ophelia started as a surface low pressure area west of the Azores around 6 October. An upper-atmosphere trough had been pushed south from the midlatitudes, and the accompanying divergence east of the trough pulled air away from the ground, creating the low (Stewart, 2018). The SSTs under the area were only marginally high enough for development (see Figure 2a) though when combined with lower temperatures aloft allowed it to strengthen, and by 18Z 11 October Ophelia had reached hurricane strength (wind speeds of >119 km/h)(Simpson and Saffir, 1974).

An approaching midlevel trough picked up the previously slow-moving storm (see Figure 2b), now struggling with increasing wind shear and decreasing SSTs (Stewart, 2018). However, Ophelia continued strengthening as it moved northeastward, becoming a Category 3 hurricane by 12Z 14 October. As the jet sent it rocketing towards Europe and into colder waters, Ophelia started its ET. Passing by the Iberian Peninsula on 15 October, strong outflow winds from Ophelia fanned wildfires in Portugal, which ended up claiming the lives of 51 people. As the storm approached Ireland, it completed its ET, but remained a powerful storm with winds of 129 km/h. Figure 2c shows the 850 hPa potential temperature at 16 Oct 12Z, just an hour after it made landfall in Ireland. The satellite image in Figure 2d is taken less than an hour later. Together they indicate that Ophelia transitioned into a Shapiro-Keyser-type ETC, which is characterized by an area of warm air separated from the bulk of the warm air by an area of cold air that wrapped around it, also known as a warm-seclusion ETC (Shapiro & Keyser, 1990). Ophelia continued bringing strongly stormy conditions across Ireland, and then onto Scotland and Norway before dissipating against the latter's mountainous terrain (Stewart, 2018).

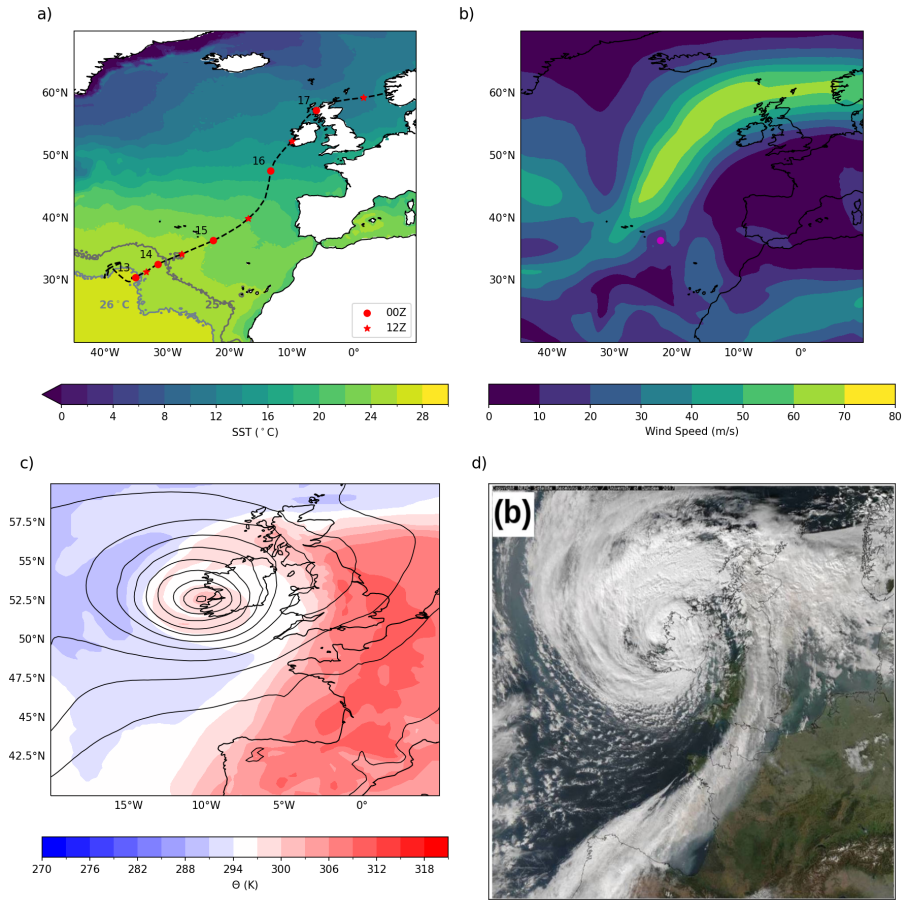

Figure 2: Composites of Hurricane Ophelia, (a), (b), (c) from GFS analysis, (d) from Rantanen et al. (2020). (a): National Hurricane Center best track with markers for the 00Z and 12Z positions of Ophelia indicated by dots and stars respectively, with day indicated at 00Z position, over sea surface temperature at 11 Oct. 00Z with the 25 and 26 °C isotherms contoured. (b): 200 hPa wind speed at 15 Oct. 00Z with the best track position of Ophelia indicated by the pink dot. (c): 850 hPa potential temperature (shading) with mean sea level pressure contours at 16 Oct. 12Z. (d): Satellite image of Ophelia at 16 Oct. 12:43Z.

3 Methods

3.1 General Approach

In this study we start by examining three global analysis datasets (ERA5, GFS, and OPER; see Section 3.2) to determine which simulates Ophelia most accurately. We then use that dataset to force two series of simulations in a regional model (RACMO; see Section 3.4); first, a series of simulations under current climate conditions initialized every 24 hours. Based on cyclone track and central pressure profiles for each simulation we select the initialization time that most accurately models Ophelia, with special consideration given to how it models the tropical phase of the storm. Second, we apply a series of uniform temperature forcings to simulate alternate climates, and examine how Ophelia changes in alternate climates. We accomplish this through examining cyclone track, central pressure, wind speed, as well as the progression of the ET. Lastly we examine the changing impacts of Ophelia.

3.2 Analysis Datasets

Analysis datasets and their close cousins reanalysis datasets are created by feeding a climate model with data assimilated from many sources. Observations from places such as weather stations, buoys, radar, satellites, and ships are combined with past weather forecasts and fed into the data assimilation program, which adjusts the model in space and time to get the closest match to the observations. Analysis and reanalysis datasets differ in one key aspect: reanalysis data is run with the same model version over the whole length of the dataset, which can be decades long, whereas analysis datasets are made of the archived analyses from the model version that was being used at that time. This distinction only becomes important if model versions are updated partway through a study, which did not happen in our case.

To determine which analysis dataset is best to use as boundary forcing in RACMO, we compare the ECMWF fifth generation reanalysis (ERA5; Hersbach et al., 2020), and the National Centers for Environmental Prediction operational Global Forecast System analysis (GFS; National Centers For Environmental Prediction/National Weather Service/NOAA/U.S. Department Of Commerce, 2015). Both have 0.25° horizontal resolution, with hourly data for ERA5 and six-hourly data for GFS. We also compare these datasets to the Operational ECMWF analysis (OPER; ECMWF, 2017), which is a 0.1° spatial resolution dataset with a temporal resolution of six hours, to examine if a higher resolution dataset more closely replicates the observations. We evaluate the datasets based on cyclone track, central pressure, and equivalent potential temperature cross-sections.

Despite that the ERA5 and GFS are finer resolution than most of the other analysis datasets currently available, Davis (2018) found that 0.25° is still too coarse to properly model especially the strongest TCs. These datasets are therefore used to force RACMO (see Section 3.4). We used several variables from each dataset, both to examine Ophelia and force RACMO simulations: temperature, relative humidity (RH), u and v wind, and geopotential height, all on pressure levels between 100-1000 hPa. We also used mean sea level pressure (MSLP) and surface temperature.

3.3 Observational Data

Our analysis data and model simulations are compared to the International Best Track Archive for Climate Stewardship (IBTrACS) dataset, or the "best-track" data (Knapp et al., 2010). Because of Ophelia's location in the North Atlantic, this data comes from the US National Hurricane Center (NHC). This dataset includes 3-hourly longitude/latitude positions of the eye (°), 6-hourly 10-meter 1-minute averaged wind speed (kt), 3-hourly mean sea level pressure (mb), and 3-hourly wind radius (nmile) data, as well as flags for status (low, tropical storm, hurricane, extratropical, etc), Saffir-Simpson Category (1-5), among others, and is used as observational data. Figure 2a shows the IBTrACS best track for Ophelia. Figure 3 shows the best track minimum central pressure profile found in IBTrACS for Hurricane Ophelia, based on the various types of pressure measurements taken. In this case, the data is all remote/satellite based as there were no in-situ measurements, largely due to Ophelia's position far away from the United States.

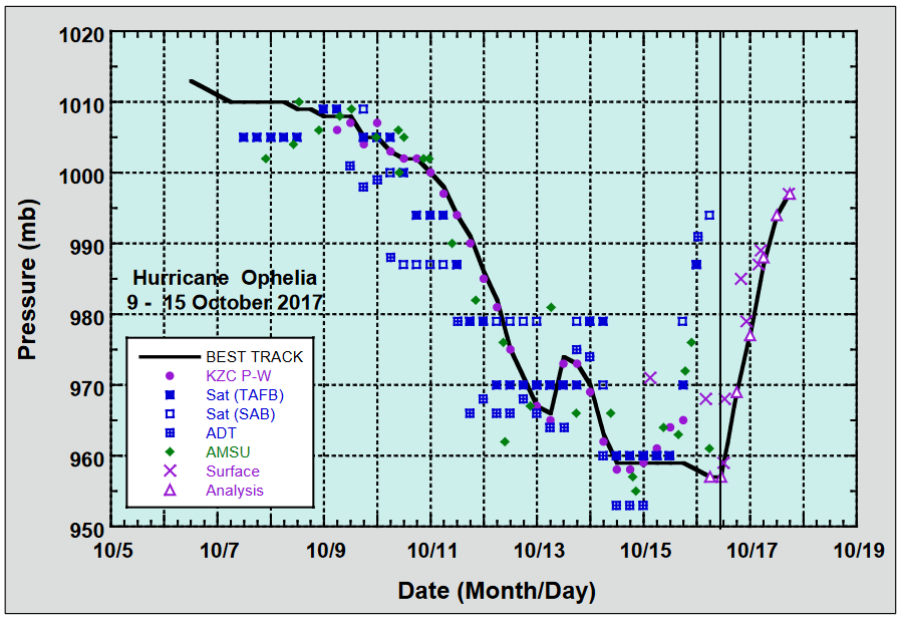

Figure 3: Hurricane Ophelia mean sea level pressure observations from various sources, overlaid with IBTrACS best track minimum central pressure profile. From Stewart (2018).

3.4 Model

3.4.1 RACMO Description

In this study, we use the Regional Atmosphere Climate Model (RACMO; van Meijgaard et al., 2012a). This model was developed by the Royal Netherlands Meteorological Institute (KNMI) and has been used with success in studies in Western Europe and Greenland, as well as for TCs in the Caribbean (Dullaart et al., in press; Luu et al., 2023; Noël et al., 2015). RACMO is a hydrostatic model with a spatial resolution of 12 x 12 km, with model physics based on ECMWF IFS Cy33r1 but an adjusted boundary layer scheme (Saarinen, 2004; van Meijgaard et al., 2012b). Our greenhouse gas concentrations are taken from CMIP5 simulations for October of 2017, and remain the same for all simulations (Taylor et al., 2012). See Appendix A for the detailed specifications.

We run RACMO over the domain pictured in Figure 4. Our choice of domain is a balancing act: capturing the entirety of Ophelia's track but also giving enough room to capture the jet stream and other upstream processes that influence Ophelia's path. At the same time this domain ensures the simulations do not become too computationally expensive or give the storm freedom to take a wildly different path. This domain choice also gives our model a chance to 'spin up' the input from the boundary conditions; the 200 hPa wind speeds on the right hand side of the domain, which are downstream thanks to the predominant westerly flow, are consistently stronger than those on the left (see Figure S1).

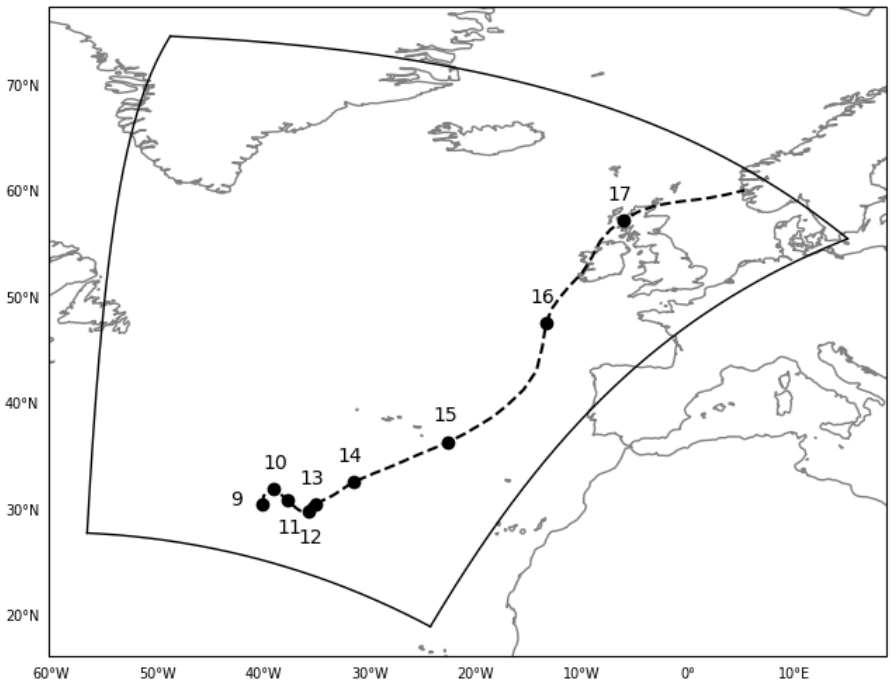

Figure 4: RACMO domain bounds with the IBTrACS best track for Ophelia during 9-18 October 2017. Markers indicate daily 00Z positions.

3.4.2 Simulation of Current Climate

We first run a set of numerical simulations of Ophelia based on the unchanged GFS boundary data, our 'current climate' simulations. Starting at 9 Oct 00Z, simulations are initialized every 24 hours until 14 Oct 00Z. Initially, the model is given 3-D forcing throughout the domain, but at later timesteps is only forced at the boundaries. Each simulation is examined for how well it simulates Ophelia by examining track placement and central pressure profiles, with special focus on the tropical development. The selected initialization time is then used for the simulation of alternate climates.

3.4.3 Simulation of Alternate Climate

We simulate seven alternate climate scenarios, each based on a uniform ΔT added to current climate forcing, following Dullaart et al. (in press). Starting with a control simulation (applied temperature forcing of 0 °C) we simulate two scenarios of a cooler climate (-2 °C and -1°C) and four scenarios of a warmer climate (+1 °C, +2 °C, +3 °C, and +4 °C).

The one constraint we add is keeping the RH constant despite the temperature change. This is consistent with global climate model study findings that RH will not change drastically with global warming scenarios (Colman and McAvaney, 1997; Held and Soden, 2000; Held and Soden, 2006).

3.5 Cyclone Tracking

3.5.1 Tracking Algorithm

Unlike in studies such as B2015 where large datasets with many TCs across decades are used, our single case allows us to use a simple cyclone tracking algorithm to find the location of Ophelia at each timestep. Figure 5 shows a conceptual diagram of the process.

First the IBTrACS latitude/longitude position of the eye at the start of the simulation is used as a guess for the initial position of the cyclone. The algorithm then searches the MSLP field in an 8° x 8° box centered on that guess for the local MSLP minimum. The position of the minimum is taken as the eye position at that timestep and the coordinates are saved, along with the MSLP value. This saved position then becomes the position guess for the next timestep, and the process is repeated throughout the rest of the dataset. The IBTrACS data is used as an initial guess to prevent the algorithm from tracking other low pressure systems also present in the simulation, but is not used beyond that so as to avoid influencing the chosen track.

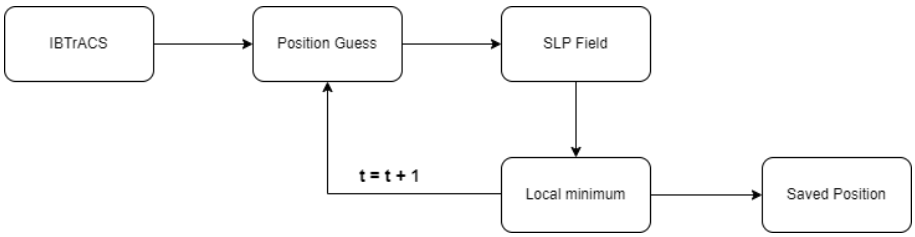

Figure 5: Conceptual flowchart of the cyclone tracking algorithm.

3.5.2 Error Metrics

We use several metrics to determine how closely the analysis datasets and RACMO model the storm. One of these is track error. This is a metric used among others by the NHC to measure the quality of their modelled track. The track error (E_T) is defined by the NHC as the great-circle distance between the cyclone forecast position and the best track position at the forecast verification time ("National Hurricane Center Forecast Verification", n.d). We calculate this using the haversine equation:

$$E_T = 2r \arcsin \sqrt{\sin^2 \frac{\Delta\phi}{2} + \cos\phi_1 * cos\phi_2 * \sin^2 \frac{\Delta\lambda}{2}} \tag{1}$$

where $r = 6371$ km, ϕ_1 and ϕ_2 are the latitudes of the two positions, $\Delta\phi$ the distance between the latitudes of the two positions (in degrees), and $\Delta\lambda$ the distance between the longitudes of the two positions (in degrees). The greater the E_T, the further the modelled position is from the best-track position.

Another error metric we use is the Root Mean Square Error (RMSE). RMSE is a measure of how well the modelled data fits to the observations, by taking the mean of the squared difference between the observations and the model output:

$$RMSE = \sqrt{\frac{\sum_{i=1}^{N}(x_{m(i)} - x_{o(i)})^2}{N}} \tag{2}$$

where N is the number of data points, x_m is the modelled data, x_o is the observed data, both at timestep i. Lower values of RMSE indicate the modelled data has a better fit to the observations.

3.6 Cyclone Metrics

3.6.1 Equivalent Potential Temperature

Equivalent potential temperature (EPT) is an enhanced potential temperature metric. Whereas ordinary potential temperature θ only takes into account the dry adiabatic warming or cooling, EPT or θ_E additionally considers the temperature change if all the water in the air parcel were to condense - releasing all the latent heat stored within. As a TC is essentially a latent heat engine, this is important to take into consideration. We use Bolton's formula (Bolton, 1980) which first

calculates the lifting condensation level (LCL) temperature (T_L), then the potential temperature of dry air at LCL (θ_{DL}), and from there EPT (θ_E):

$$T_L = \frac{1}{\frac{1}{T_D - 56} + \frac{\ln(T/T_D)}{800}} + 56 \tag{3}$$

$$\theta_{DL} = T\left(\frac{1000}{p-e}\right)^{0.2854}\left(\frac{T}{T_L}\right)^{0.28r} \tag{4}$$

$$\theta_E = \theta_{DL}\exp\left[\left(\frac{3.036}{T_L} - 0.00178\right) \times r(1 + 0.448r)\right] \tag{5}$$

where the variables are defined in Table 1.

Table 1: Variable definitions

Variable	Definition	Unit
T_L	Temperature at LCL	K
θ_{DL}	Potential Temperature at LCL	K
θ_E	Equivalent Potential Temperature	K
T_D	Dewpoint Temperature	K
T	Temperature	K
p	Pressure	Pa
e	Saturation Vapour Pressure	Pa
r	Saturation Mixing Ratio	g kg^{-1}

3.6.2 Wind Footprint and Extent

A wind footprint map is a visualization of the maximum winds experienced at every gridcell over the lifetime of a storm, on one level, often at or near the surface. This become a map of where the strongest winds were present, as a sort of 'footprint' left behind by the storm winds. We use the maximum 10m winds over the length of our simulation to examine the impacts to land.

In order to determine the simulation-length spatial extent of strong winds, we use a modified version of this wind footprint. Due to the presence of another low-pressure system in the North Atlantic before Ophelia, there is a substantial area of high winds not associated with the hurricane. To remove the influence of this and potentially other outside sources of high winds, we extract the winds in a 30° x 30° box centered on Ophelia's eye latitude/longitude at every time step. The maximum wind over the simulation is found for each grid cell, and the number of gridcells exceeding the threshold value is multiplied by the area of one gridcell to find the total extent of the strong winds.

3.7 Quantifying Extratropical Transition

3.7.1 Extratropical Transition

The NHC indicated that Ophelia had completed ET and was a PTC starting from 16 Oct. 00Z (Stewart, 2018). However, this does not tell us when ET started nor how the ET progressed. Knowing where the storm is in its transition is an important aspect of predicting what the impacts will be. We employ several techniques which explore ET start and end, as well as what occurs during the transition, as the exact progression of the transition varies with every storm.

3.7.2 Cyclone Phase Space Analysis

Cyclone phase space (CPS) analysis is a technique used to examine the structure of TCs and ETCs, as well as quantify ET. Hart (2003) introduced these now eponymous diagrams, and they have been used with success in many studies (Dekker et al., 2018; Haarsma et al., 2013; E. Jones et al., 2024; Kitabatake, 2011). Their relative simplicity allows them to be used in many different situations and datasets – this method uses only the geopotential height on pressure levels between 300 and 900 hPa. Here we offer a brief explanation and we direct readers to Hart (2003) for more details.

CPS diagrams examine two main features that change during ET: the horizontal thermal asymmetry (B) and the thermal wind ($-V_T$), which is divided into upper thermal wind ($-V_T^U$) and lower thermal wind ($-V_T^L$).

Horizontal thermal asymmetry is officially defined in Hart (2003) as "the storm-motion-relative 900–600hPa thickness asymmetry across the cyclone within 500km radius":

$$B = h(\overline{Z_{600\,hPa} - Z_{900\,hPa}}|_R - \overline{Z_{600\,hPa} - Z_{900\,hPa}}|_L)$$

where h is a parameter to account for hemispheric differences (+1 for the northern hemisphere, -1 for the southern hemisphere), Z is the isobaric height, $_R$ and $_L$ indicate the halves to the right and left of the storm respectively. Horizontal thermal asymmetry is nearly non-existent in a TC ($B \approx 0$) due to their radial profile with a warm center and cool exterior. In an ETC this is not the case, as the frontal nature of the storm means one side will be significantly cooler than the other and thus geopotentially thinner. Evans and Hart (2003) (hereafter EH2003) determined that for North Atlantic storms, ET starts when the asymmetry parameter B is greater than 10 m.

The upper and lower thermal wind are calculated as:

$$-V_T = \frac{\partial(\Delta Z)}{\partial(\ln p)}$$

where p is pressure and ΔZ is the height perturbation on that pressure level ($\Delta Z = Z_{MAX} - Z_{MIN}$). The thermal wind can be used as an approximation to the cyclone isobaric height gradient, which is the height perturbation on a pressure level, ΔZ, in a 500 km radius from the center of the cyclone. This is related to the lower-troposphere thermal wind, as a warm core system will have a positive $-V_T^L$ because the perturbation at 900 hPa would be larger than at 600 hPa.

In Hart (2003) a 50 hPa vertical interpolation is used, but due to the lack of pressure levels in our data, we calculate $-V_T$ as a simple difference between the upper and lower bounds (300 and 600 hPa for $-V_T^U$ and 600 and 900 hPa for $-V_T^L$). As we do not have data at 600 or 900 hPa, these are calculated as linear interpolations between 500 and 700 hPa and 850 and 925 hPa respectively.

Positive values of the thermal wind indicate a storm core that is warm compared to the environment, and negative values indicate a storm core that is cold compared to the environment. This relationship allows us to study ET, as generally TCs have warm cores and ETCs have cold cores.

The calculated B, $-V_T^U$, and $-V_T^L$ data was smoothed in post-processing to remove noise present due to the coarse resolution in especially the vertical dimension. Hart (2003) did his processing in a similar manner, though we take a 12-hour convolution rather than a 24-hour running mean to preserve more data at the edges of our domain.

3.7.3 Isobaric Height Gradient Profiles

We quantify the end of ET by following the definition of EH2003: ET is completed when the 900-600 hPa cyclone isobaric height gradient corresponds to that of a cold-core storm (increasing with height) rather than a warm core (decreasing with height). This can also be interpreted as a negative value of $-V_T^L$.

An example from EH2003 is given in Figure 6, where during the ET of Hurricane Floyd (1999) several vertical cross-sections are taken of Z_{MAX}–Z_{MIN} that show this warm-to-cold-core transition. EH2003 base this only on the 900-600 hPa profile rather than the full atmosphere because the upper atmosphere can become cold-core as the convection becomes shallower, but still be very much present in the lower levels of the atmosphere.

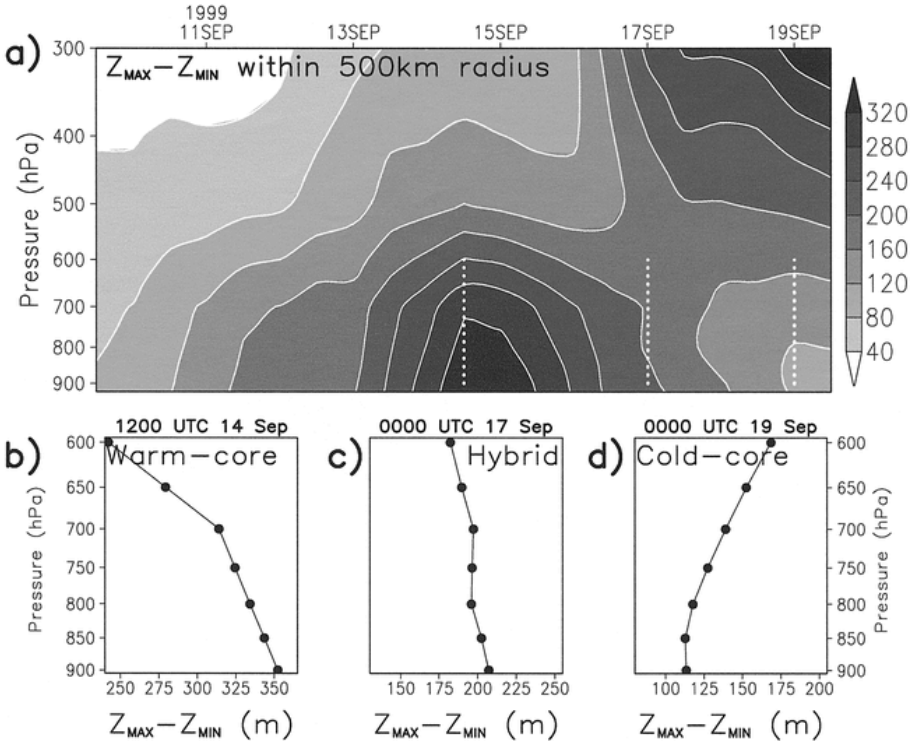

Figure 6: The warm-to-cold-core evolution during the extratropical transition of Hurricane Floyd (1999). (a) Time–height cross section of Z_{MAX}–Z_{MIN} (m) as interpreted by the 1° × 1° NOGAPS analyses. Vertical profiles of Z_{MAX}–Z_{MIN} between 600 and 900 hPa at three times are given for (b) tropical phase at 1200 UTC 14 Sep, (c) hybrid phase nearing transition completion at 0000 UTC 17 Sep, and (d) extratropical phase at 0000 UTC 19 Sep. From Evans and Hart (2003).

4 Results and Discussion

4.1 Analysis Datasets

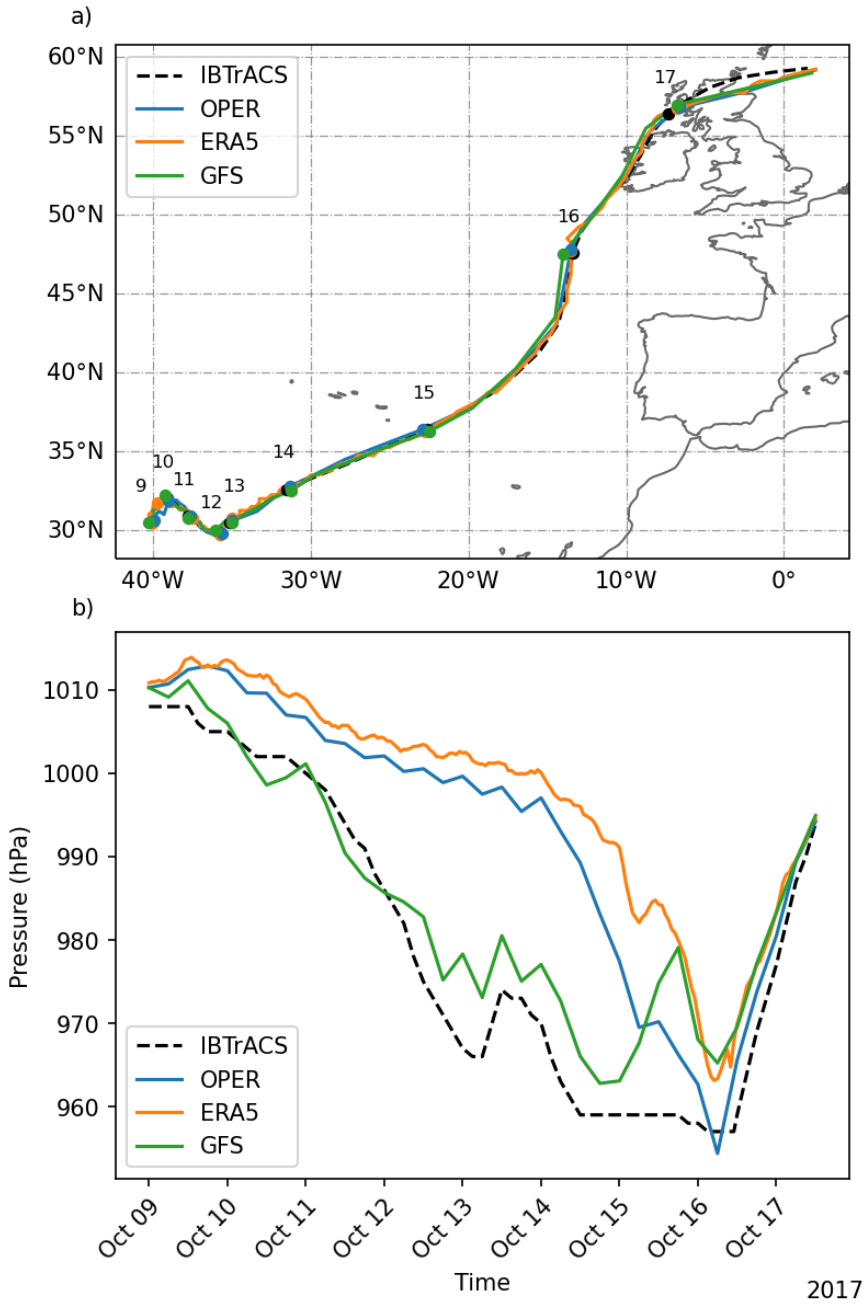

Figure 7: Track (a) and central pressure minimum (b) of Hurricane Ophelia for the three analysis datasets: OPER, ERA5, and GFS.

Figure 7 shows the plotted track and central pressure minimum timeseries for Hurricane Ophelia in the three analysis datasets: GFS, ERA5, and OPER, compared to the observations from IBTrACS. The agreement between the dataset track and the observed track is very good for each of the datasets. There is some variation on 17 Oct, where all three datasets take a more southerly route than the observations would suggest. This may be because Ophelia is at that point a broader low which makes it harder to pinpoint an exact central minimum as with a TC. Table 2 shows the mean track error for each of the datasets. GFS had lower mean track error than ERA5 and OPER, but only by about 5 km. In comparison, the NHC 12h forecast track error for Ophelia was 36.7 km (Stewart, 2018).

Table 2: Mean track error (km), maximum central pressure deviation (hPa), and central pressure root mean square error (RMSE) (hPa) for the three datasets, all compared to IBTrACS observations.

Dataset	Mean Track Error (km)	Maximum Central Pressure Deviation (hPa)	Central Pressure RMSE (hPa)
OPER	28.8	+32.6	14.8
ERA5	28.3	+37.0	18.3
GFS	23.2	+20.1	6.4

Despite the accurate tracks, our results show that all three datasets have difficulty reproducing Ophelia's intensity, with the largest deviation being an overestimation of the central pressure of 37.0 hPa by ERA5 (Figure 7b). We find this large error strongly in the tropical (TC) phase of the storm, but find much better agreement with the observations in the extratropical (ETC) phase.

This aligns with findings that while current models have substantially improved their ability to forecast track in the last decades, there has been much more difficulty in accurately modelling TC intensity (DeMaria et al., 2014). The NHC also cites difficulties in establishing the actual strength of the storm (Stewart, 2018). This overestimation of Ophelia's central pressure was also encountered by Rantanen et al. (2020).

Interestingly, difficulty modelling TC intensity does not appear to be solely attributable to coarse resolution. While the 0.1° OPER does have a lower central pressure RMSE than the 0.25° ERA5, showing that resolution does play a role, both ECMWF-based models perform substantially worse than the 0.25° GFS (Table 2). GFS has the lowest central pressure RMSE at 6.4 hPa as well as the lowest maximum central pressure deviation (20.1 hPa). Visually, the pressure profile of Ophelia in the GFS dataset also corresponds better to the observations. These findings align with known results on with ECMWF-based tropical cyclone studies; Majumdar et al. (2023) used a 4 km model and still found that the central pressure minima of their TCs were overestimated, especially when undergoing rapid intensification.

We also compare vertical cross-sections of EPT through Ophelia's core for ERA5 and GFS, taken at 14 Oct 00Z (Figure 8). In the GFS, Ophelia's core has a maximum EPT of 359 K, compared to 348 K in ERA5. Higher values of EPT indicate greater potential for latent heat release-driven warming, which is indicative of a stronger storm. As these cross-sections are taken 12 hours before Ophelia intensified into a major hurricane, we expect to see a core high in EPT. Additionally, ERA5 shows a distinct decrease in EPT at the midlevels - as though the convection is not proceeding fully from the bottom of the atmosphere to the top.

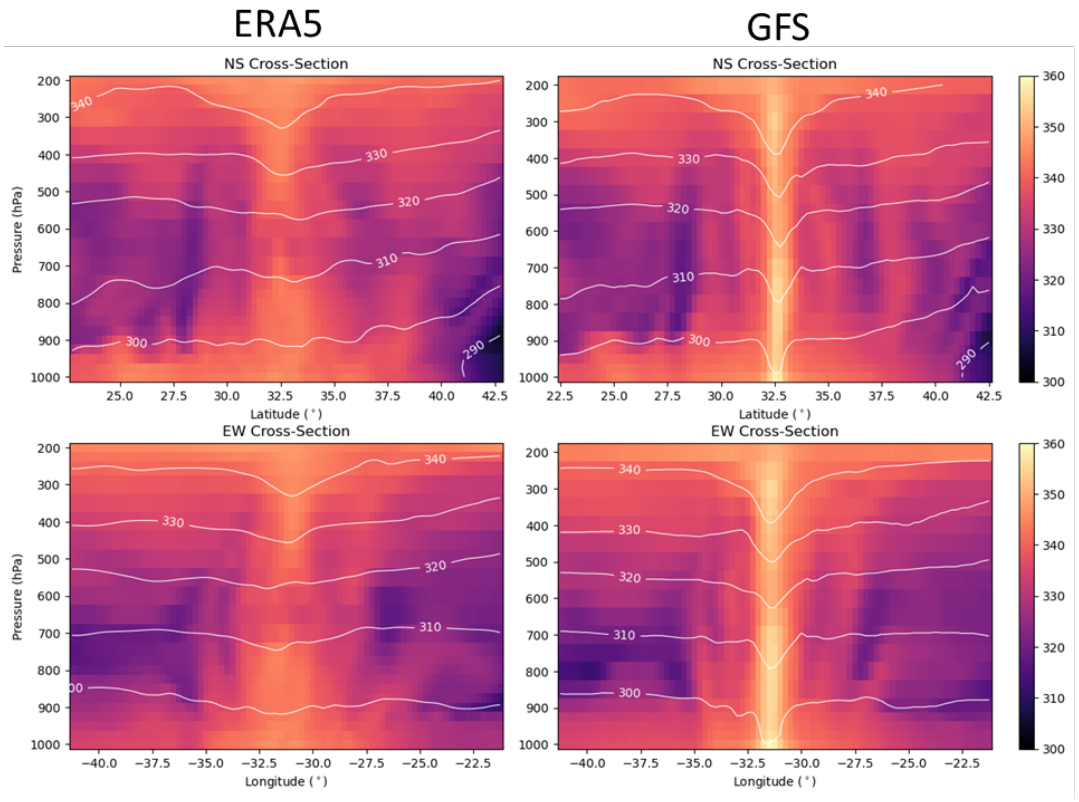

Figure 8: Equivalent potential temperature cross-sections (shaded) with potential temperature contour lines (white) for Hurricane Ophelia from the ERA5 (left) and GFS (right) for north-south (NS, top) and east-west (EW, bottom) at 14 Oct 00Z.

Furthermore, the potential temperature contours in the GFS cross-sections show a dip in the core that is basically absent from the ERA5 cross-sections. These dips indicates a core that is distinctly warmer than the surrounding regions, due to more latent heat release. This process is enhanced in GFS over ERA5. These results correspond well with the central pressure profiles in (Figure 7), which show two different storms at this time: a weak low in the ERA5 (1000.1 hPa), and an already strong hurricane in the GFS (977.1 hPa).

In summary, the GFS dataset more accurately simulates Ophelia's track, central pressure profile, and thermal structure than ERA5 or OPER. Crucially for this study, it also does so in the tropical phase of the storm. We focus on the tropical phase of the storm since this is where the storm does most of its intensifying - a storm that transitions as a strong TC into a strong PTC is a different storm than a weak TC that rapidly intensifies during ET.

4.2 RACMO Simulations

4.2.1 Current Climate

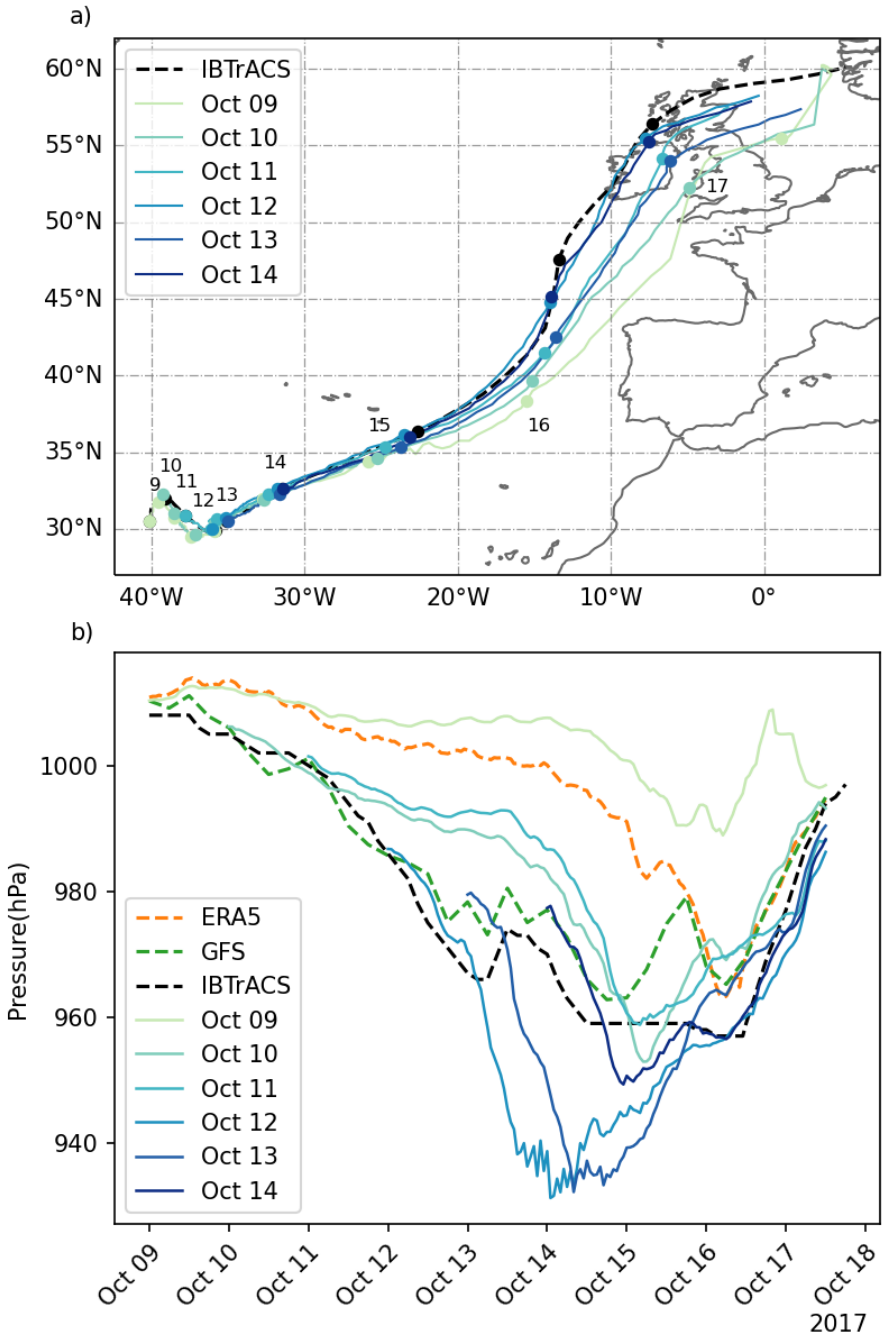

Figure 9: Track (a) and central pressure minimum (b) of Hurricane Ophelia for the downscaled RACMO simulations with GFS boundaries. Each is initialized at 00Z on the day labelled and compared to observations from IBTrACS. Also included in (b) are the ERA5 and GFS central pressure profiles.

Figure 9a shows the tracks for the GFS-driven downscaled current climate RACMO simulations, each initialized at 00Z on the day labeled. The tracks show more spread than the tracks in the analysis datasets as the mean track error ranges from 108.8 km to 278.0 km, from initializations 12 and 9 October respectively (Table 3). This is consistent with findings from Majumdar et al. (2023), who found that even with a 4 km model, track error was consistently larger with TCs that are initially weak storms than those that are initialized as hurricanes.

Table 3: Mean track error (km), cumulative track error, initial central pressure, and maximum central pressure deviation for each initialization, all compared to IBTrACS observations.

Initialization date (Oct 2017)	Mean Track Error (km)	Cumulative Track Error (km)	Initial Central Pressure (hPa)	Maximum Central Pressure Deviation (hPa)
09	278.0	19183.6	1010.3	+46.5
10	277.5	16929.0	1006.2	+22.8
11	211.6	11216.7	1001.5	+26.4
12	108.8	4895.9	986.7	-36.7
13	230.7	8536.7	979.5	-24.6
14	164.8	4778.5	977.4	+9.1

Initially the tracks show good agreement, especially laterally - there is little movement perpendicular to the track direction. The markers at 15 October however, show a large spread in along-track position, indicating that despite the lateral clustering, the track error is growing due to an underestimation of storm translation speed. Figure 10 illustrates this through the evolution of the track error. Regardless of initialization time, 14-15 October seems to be the point in time where the tracks start to diverge more rapidly, with a visible increase in track error.

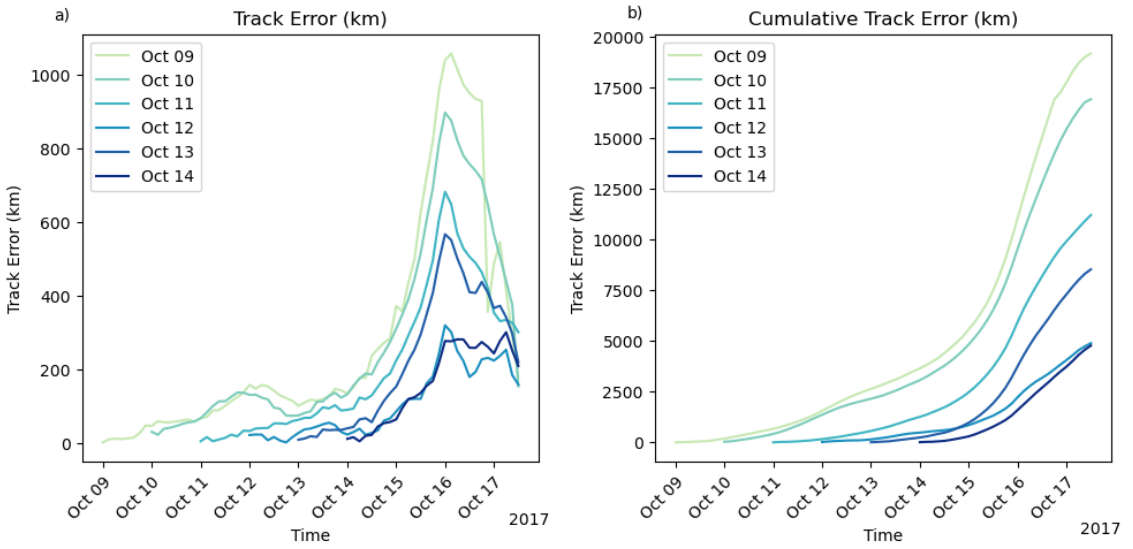

Figure 10: Track error (a) and cumulative track error (b) of downscaled RACMO simulations of Hurricane Ophelia, with GFS boundaries, initialized at 24 hour intervals, compared to observations from IBTrACS.

The track error direction all falls to the right of the observed track, indicating that the simulated storms do not turn northwards rapidly enough. This northwards turn should take place on 15 October, and only the tracks of the 12 and 14 October simulations turn enough to match the observations. No sufficient cause was found to explain these differences, though several driving factors were examined. The 200 hPa wind shows too little variability between simulations to explain the difference in position. The MSLP does not show any signs of a large-scale pressure gradient that would propel Ophelia further north in the 12 and 14 October simulations but not in the others.

Visually, the tracks of the simulations initialized on 12 and 14 October show the best agreement with the IBTrACS observations. They also have the lowest mean track error (108.8 and 164.8 km) and the lowest cumulative track error (4895.9 and 4778.5 km) (Table 3). This last metric is especially impressive for the 12 October initialization, as it ran 48 hours longer than the 14 October initialization. Figure 10b shows how the error remained consistently low for the 12 October initialization.

Figure 9b shows the central pressure profiles of the current-climate RACMO simulations, as well as the central pressure profiles of the ERA5 and GFS datasets, and the observations from IBTrACS. The simulations exhibit a large range of different profiles, with central pressure deviations ranging from -36.7 to +46.5 (initializations 12 and 9 October respectively; see Table 3).

The simulations initialized before 12 October overestimate the central pressure, indicating a storm that is weaker than the observations. This is especially present in the tropical phase of the storm, and is quite similar to the profiles we saw in the ERA5/OPER datasets. These three simulations are all started at relatively high central pressures (all above 1000 hPa, whereas the others are less than 990 hPa). Majumdar et al. (2023) found that simulations that started with a weaker storm had, on average, a higher central pressure bias than simulations that started with a stronger storm.

The simulations initialized on 12 and 13 October experience the opposite problem: they overestimate the strength of the storm, far surpassing the minimum pressure of the observations (maximum deviations of -36.7 and -24.6 hPa respectively). However, they do capture the strengthening of the storm in its tropical phase, something the other simulations do not manage. This extreme strengthening is also likely associated with the initialization pressure as found in Majumdar et al. (2023).

While the 14 October simulation shows the best agreement with the observations in terms of cumulative track error and both MSLP metrics (see Table 3), its late initialization time does not allow us to study the tropical phase of the storm sufficiently before ET starts. In the end, October 12 is determined to be the best initialization time to study Ophelia in RACMO. Its track error is substantially lower than the initialization times around it, and an overly stronger storm is preferred to a storm that barely exists.

4.2.2 Alternate Climate

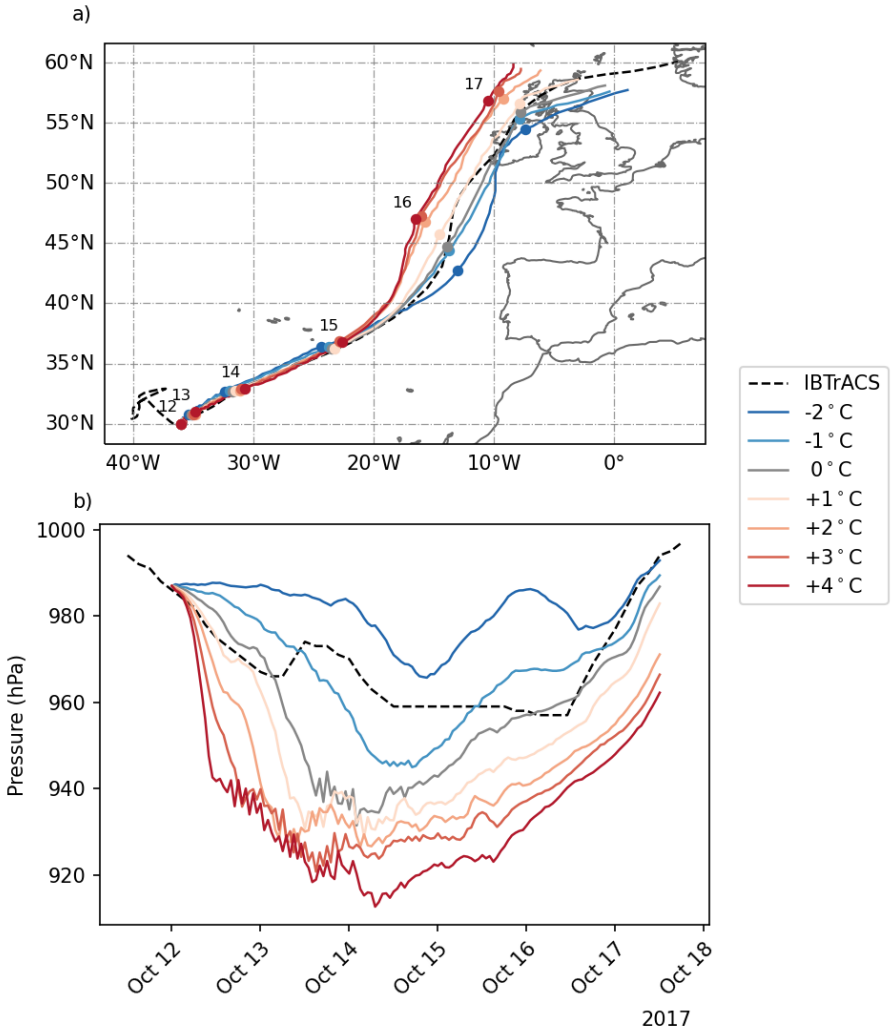

Figure 11: Track (a) and central pressure minimum profiles (b) of Hurricane Ophelia for the alternate climate downscaled RACMO simulations with GFS boundaries, initialized at 00Z 12 October 2017. (a) Circles plotted at 00Z of the date indicated.

Figure 11a shows the track of Hurricane Ophelia in each alternate climate simulation. The tracks initially show high levels of lateral clustering, but after 15 October they diverge. Unlike the current climate simulations in Section 4.2.1, there is a clear pattern to the placement of these tracks. Simulations with higher temperature forcing track further northwest than those with lower temperature forcing. This difference occurs as a result of an earlier, stronger northwards turn and peaks at 15 Oct 23Z, with Ophelia being 559 km further northwest in the +4 °C simulation than in the -2 °C simulation. This is an average of about 90 km further northwest per degree of warming. The three warmest simulations (+2 °C, +3 °C, and +4 °C) even have Ophelia not making landfall, but passing by off the west coast.

While the simulations show a low level of lateral track divergence before 15 October, there is a divergence in along-track location already present. Similarly to the tracks in the previous simulation, we see this in the marker clustering, as well as the rising track error (Figure S2a). This is due to a difference in translation speed, with the storm in simulations with higher temperature forcing moving faster and vice versa for simulations with lower temperature forcing (see Figure S3).

This increase in translation speed with temperature can be attributed to an earlier interaction with the jet stream.Radu et al. (2014) found that the size of a TC increases proportionally to the surface latent heat flux, which over the ocean is determined by the SSTs. Since the SSTs are also forced by the applied ΔT, in the warmer simulations Ophelia would then grow larger. This allows

Table 4: Minimum central pressure, maximum central pressure deviation, and maximum 10m wind speed for each alternate climate scenario, compared to IBTrACS observations.

Temperature Forcing (°C)	Minimum Central Pressure (hPa)	Maximum Central Pressure Deviation (hPa)	Maximum 10m Wind Speed (m/s)
-2	965.7	+28.1	43.0
-1	944.9	-15.0	49.2
0	931.4	-34.9	54.8
+1	928.7	-43.3	55.4
+2	926.5	-44.0	57.7
+3	920.7	-46.5	59.4
+4	912.6	-51.0	59.4

earlier interaction with the jet stream, giving the storm propulsion northeastward sooner than in the cooler simulations with a smaller Ophelia (see Figure S4). We also find that the upper level flow streams faster in the simulations with higher temperature forcing than in the simulations with lower temperature forcing (see Figure S1).

The central pressure profiles of the alternate climate simulations exhibit a strong linear trend: in simulations with higher temperature forcings, Ophelia has a lower central pressure (Figure 11b). The +4 °C simulation has the deepest central pressure minimum at 913 hPa, and the -2°C has the highest central pressure minimum at 966 hPa (Table 4).

The initial 24 hours of the simulations show swift intensification in most scenarios, with the warmest simulations (+2 °C, +3 °C, and +4 °C) all experiencing more than 45 hPa of intensification in that time. While this is quite fast, it is by no means extreme - 2005's Hurricane Wilma had a maximum 24-hour pressure drop of 97 hPa (Pasch et al., 2006). This intensification is explained largely by the increase in temperature. In the warmer scenarios, the SSTs are also higher. Since RACMO is an uncoupled model and thus does not have ocean feedbacks like the stirring up of cold water from below the warm surface layer, these warm SSTs provide an unending source of fuel for Ophelia, allowing it to strengthen substantially.

We ran the same alternate climate scenarios for an initialization time of 11 October 00Z, and despite the much slower storm strengthening due to underestimation of the intensity in the tropical phase, we find a very similar relationship between temperature forcing and storm intensity (Figure S5). This bolsters the robustness of the signal we see, giving confidence in our results, despite only looking at a single case study.

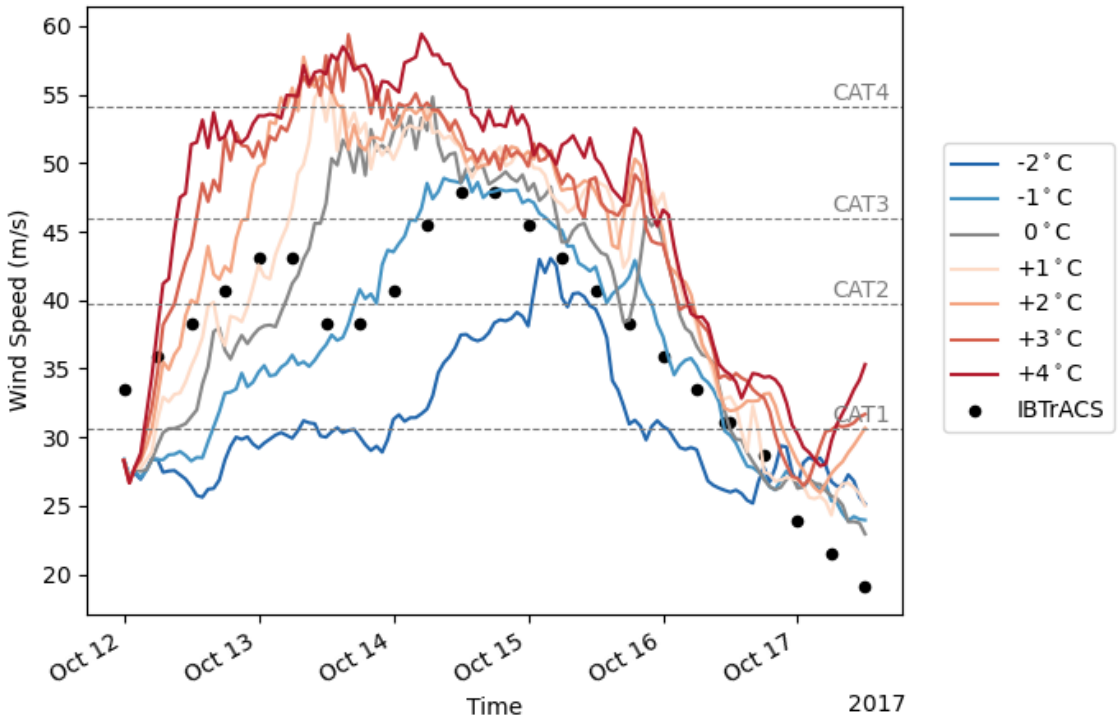

Figure 12: Maximum 10 m wind speed (m/s) for Ophelia in each of the RACMO alternate climate scenarios, compared to the observations from IBTrACS. Dashed lines mark the threshold values for the Saffir-Simpson Hurricane Scale Categories.

Wind speed is another frequently used measure of cyclone intensity. Figure 12 shows Ophelia's maximum 10m winds for each of the RACMO alternate climate scenarios. In simulations with higher temperature forcing Ophelia has an earlier increase in strong winds than in those with lower temperature forcing. It takes more than 72 hours for the -2°C simulation to reach Category 2 status, but only 7 hours for the +4°C simulation. This is consistent with the rapid intensification we saw in the central pressure profiles, as wind speed and central pressure are linked through the TC pressure-wind relationship (Chavas et al., 2017; Courtney and Knaff, 2009).

The -1°C simulation appears to agree best with the observations, with a maximum 10m wind speed of 49.1 m/s compared to 47.8 m/s in the observations. However, the simulated versions of Ophelia all miss the two-peaked pattern seen in the observations. Stewart (2018) attributes this pattern in the observations of Ophelia to an increase in wind shear in the early hours of 13 Oct, and a similar variation is also present in the pressure profiles (Figure 11). Our simulated versions of Ophelia show only minor variation in the pressure profiles at that point, so likely the wind shear that affected Ophelia in reality was not present or as impactful in the model.

All of the simulations with 0°C and higher temperature forcing have wind speeds that would classify them as Category 4 hurricanes, despite the large differences in central pressures seen in Table 4. However, not even the +4 °C crosses the 65 m/s boundary needed for Category 5 status. This is consistent with the findings of Dullaart et al. (in press) who found that RACMO simulated more Category 4 storms than occurred in reality, while greatly underestimating the number of Category 5 storms.

4.3 Extratropical Transition

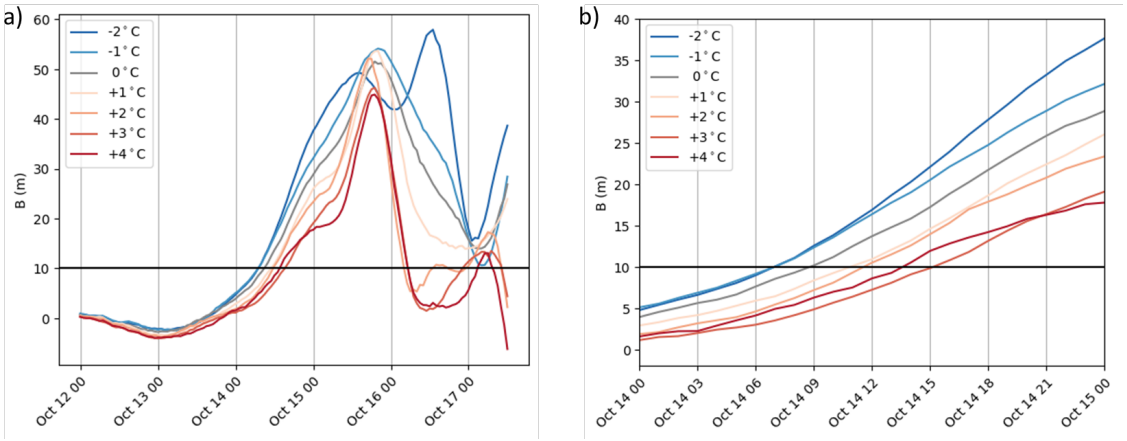

Figure 13: 900-600 hPa thickness asymmetry for the varying temperature scenarios for (a) the full length of the simulations and (b) zoomed in on the extratropical transition start.

Figure 13a shows the temporal evolution of the thermal asymmetry parameter B in Ophelia for each of the alternate climate scenarios. Based on the definition in EH2003, we can pinpoint when Ophelia's ET starts. In each scenario, B initially remains well below the ET threshold value of 10 m, as expected for a symmetric TC. All of the simulations cross the ET threshold (starting their ET) between 7 and 15 Z on October 14 (13b). In general, the scenarios with lower temperature forcing start ET earlier than the scenarios with higher temperature forcing, but there is some fluctuation, with the +4 °C simulation leading the +3 °C by almost an hour and a half, and the -2°C and -1°C simulations starting their ETs at nearly the same time. The fact that in the warmer simulations Ophelia remains symmetric for longer, means it retains its TC characteristics longer than in cooler simulations.

The asymmetry can also tell us about the progression of the ET. Figure 13a shows that the warmest simulations become less asymmetric overall than their cooler counterparts, with the +4 °C achieving only 78% of the asymmetry of the -2°C simulation (44.9 m vs 57.9 m). All simulations except the -2°C have a near-simultaneous peak in asymmetry at the end of 15 October, after which their asymmetry decreases again. The warmest simulations very quickly attain low levels of asymmetry and return to near-TC levels. What this indicates for Ophelia is that in the warmer scenarios it maintains more of its TC-like characteristics.

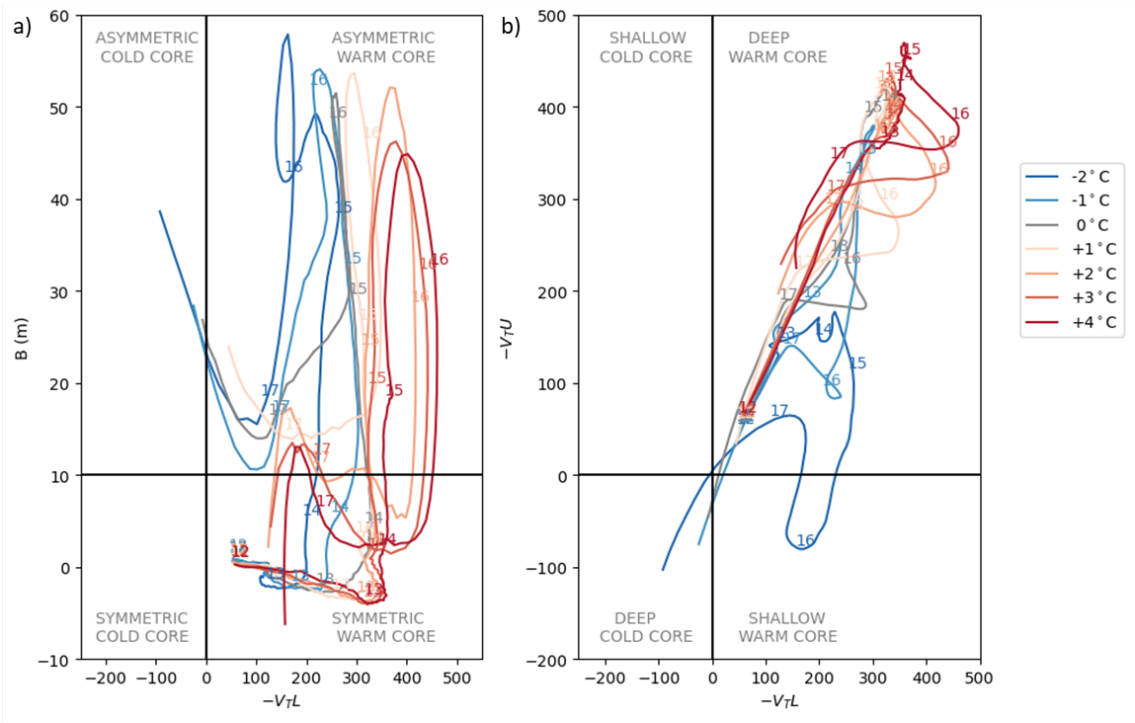

Figure 14: Hart Diagrams for the RACMO alternate climate scenarios, with (a) lower tropospheric thermal wind ($-V_T^L$) vs thickness asymmetry (B) and (b) lower tropospheric thermal wind ($-V_T^L$) vs upper tropospheric thermal wind ($-V_T^U$).

We can put this progression of ET in more context by looking at the full CPS diagrams for Ophelia. Figure 14a shows the simultaneous progression of the asymmetry and the lower level thermal wind. The simulations with higher temperature forcing have a higher $-V_T^L$ than the simulations with lower forcing, indicating their cores are warmer in the lower troposphere. This is to be expected with the ΔT we introduced, as the warmer SSTs mean more available latent heat, and thus more warming. The simulations with positive temperature forcing also continue increasing in $-V_T^L$ even after reaching peak asymmetry, and $-V_T^L$ only starts decreasing substantially in the second half of 16 October. We do not see this post-peak-asymmetry $-V_T^L$ increase in the simulations with 0°C or less temperature forcing. Rather, these remain the same or decrease in $-V_T^L$ after peak asymmetry. These increases in $-V_T^L$ in the warmer simulations may be the warm core of Ophelia, in its transition to a warm seclusion ETC, still taking up latent heat from the warm SSTs. Rantanen et al. (2020) found that diabatic heating was the dominant forcing in both the tropical and extratropical phases of Ophelia. Diabatic heating has also been shown more generally to be important in the development of warm-seclusion ETCs (Grønas, 1995).

The simulations with higher temperature forcing have a higher $-V_T^U$ as well (Figure 14b). This suggests that Ophelia's convection in the warmer scenarios is stronger, because more heat is making its way up to a higher level of the atmosphere. Here we also see the same increase of $-V_T^L$ after 15 October noted in Figure 14a, but now it is coupled to a slight decrease in $-V_T^U$ instead of the decrease in asymmetry. While the lower troposphere is warming up, the upper troposphere is actually cooling slightly. There are two processes at work here simultaneously: continued latent heating of the lower troposphere and decreased per unit area heating in the upper troposphere. The lower troposphere can continue warming through latent heat release even after ET, which helps maintain the warm-seclusion (Quitián-Hernández et al., 2020). Meanwhile the tilting of the storm column with height due to the cooler (geopotentially thinner) air to its west increases the volume of air in the core, decreasing the per unit volume heating even with the same input of energy. However this heating also starts to decrease as the storm moves over colder water. We can also attribute the eventual decrease of both $-V_T^U$ and $-V_T^L$ to the cooler-SST-driven decrease in available latent heat.

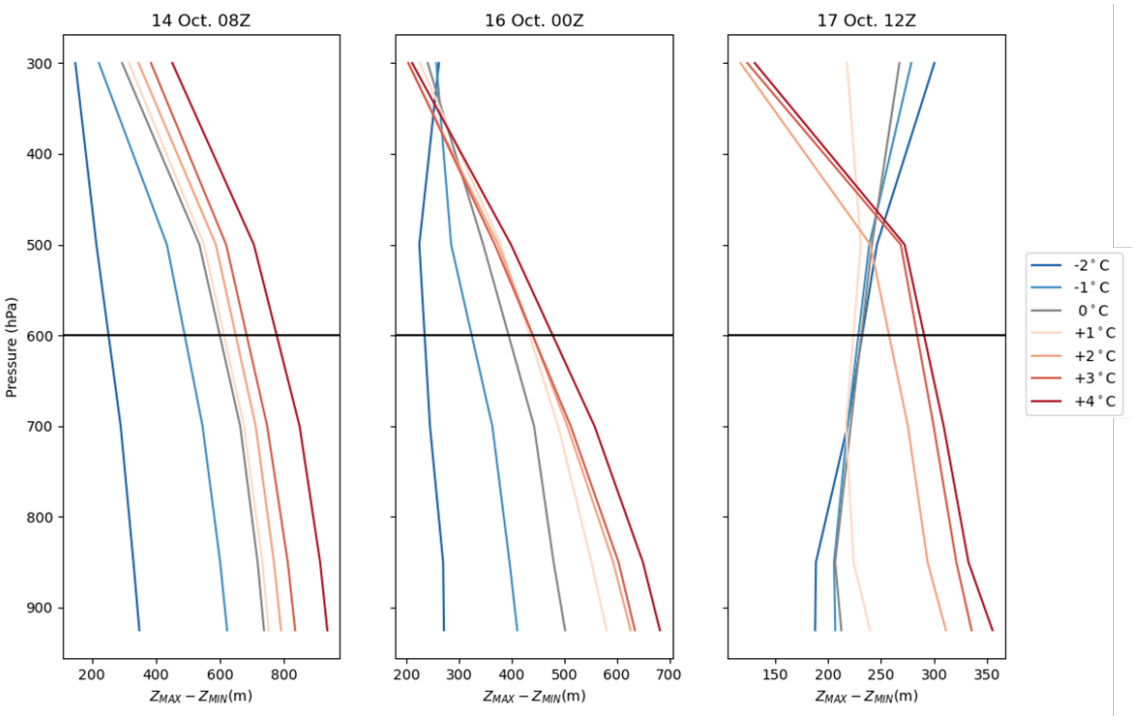

Figure 15: Isobaric height gradient profiles for each temperature scenario for the approximate start of extratropical transition (14 Oct 08Z, left), at the National Hurricane Center-determined extratropical transition completion point (16 Oct 00Z, middle), and at the end of the simulations (17 Oct 12Z, right). Note the varying x-axis.

To quantify the end of Ophelia's ET we take the second definition from EH2003 and examine the evolution of Ophelia's isobaric height gradient profiles in each alternate climate scenario (see Figure 6 and Section 3.7.3 for explanation). At the approximate start of the ET (Figure 15, left panel) Ophelia is still a TC in all scenarios, as they show a clear warm-core profile under 600 hPa. By 16 Oct 00Z, at which time Ophelia completed ET according to the NHC, the -2°C scenario has Ophelia becoming cold core in the upper levels (Figure 15, middle panel). This is an indication that the convection has become shallow and the storm is transitioning to extratropical. The convection in the -1°C scenario is also starting to become shallow but the rest of the simulations are still strongly warm core. At the end of our simulation time (17 Oct 12Z, Figure 15, right panel), the -2°C through +0°C versions of Ophelia are firmly cold core storms, while +1°C exists as a hybrid between warm and cold core, and the +2°C through +4°C still retain their warm cores.

To summarize, in warmer climates Ophelia does not finish ET but instead remains a warm-core hybrid of TC and ETC. This is in line with B2015's findings for both their case study storm Amy and other near-future PTCs.

This is dangerous for areas like Ireland which are more used to ETCs than TCs. TCs bring a different structure and impact footprint than ETCs: TCs have slight wind speed asymmetry due to the influence of the translation speed, but this is greatly increased in an ETC (S. C. Jones et al., 2003. The precipitation in an ETC also shifts to the left of the track and poleward of its location around a TC core, which as a result changes the impacts of the storm.

4.4 Impacts

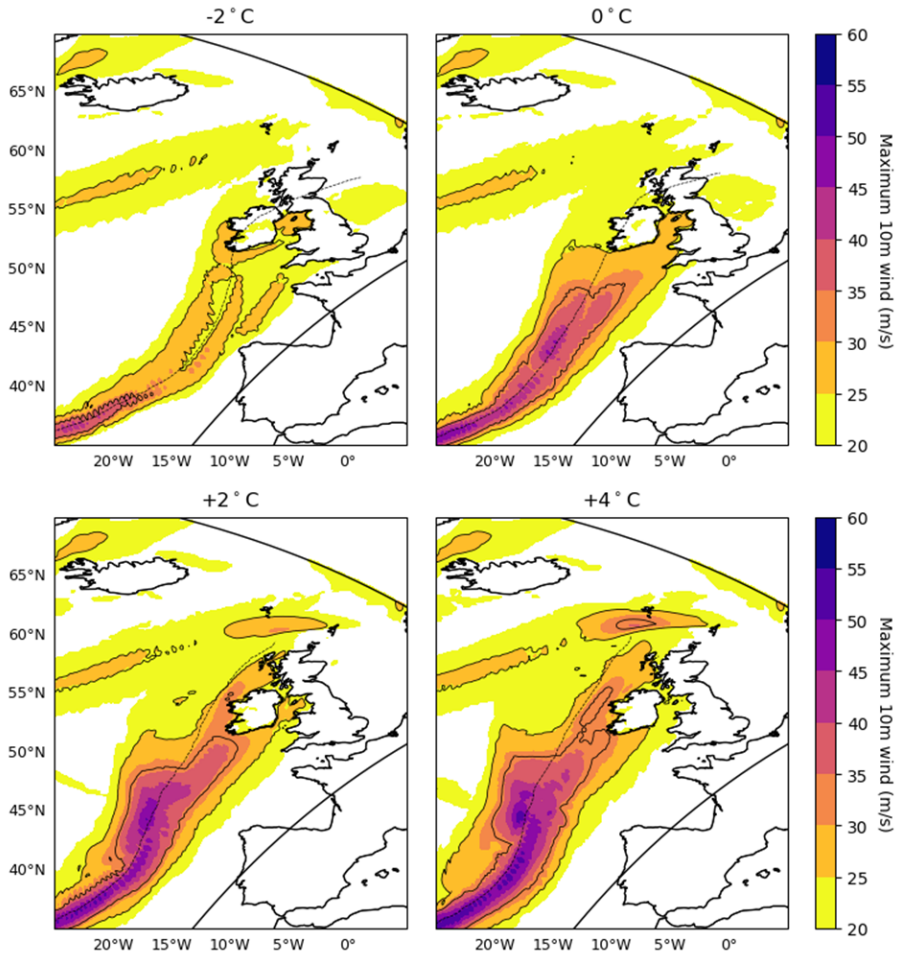

Figure 16: 10m wind footprint for Ophelia in the -2, 0, +2, and +4 °C alternate climate scenarios, with their respective tracks. Contour lines at storm-force (10 Bft, 24.7 m/s) and hurricane-force (12 Bft, 32.8 m/s). RACMO domain bounds drawn as well.

Figure 16 shows the 10m wind footprint, or the highest wind speed recorded at every grid point throughout the length of the simulation, for the storm in four of the scenarios (-2, 0, +2, and +4 °C). The overall maximum 10m wind increases with increasing temperature forcing (from 43 m/s to 59 m/s in scenarios -2 to +4°C), which is consistent with the strengthening storm we see in the decreasing central pressure profiles (Figure 11). The area affected by Ophelia's winds increases simultaneously, with both the storm-force (10 Bft or 24.7 m/s) and hurricane-force (12 Bft or 32.8 m/s) winds increasing substantially: the +4°C simulation has, respectively, areas 157% and 162% larger compared to current climate conditions (0°C; see Figure S4).

Interestingly, although the track moves westward with warmer scenarios, the winds experienced around Ireland are higher than in the scenarios where the storm hits the country directly. Figure 17a shows the 10m winds at the grid point closest to five measuring stations around Ireland, for each temperature scenario, compared to the maximum 10-minute wind speeds observed at those stations during Ophelia. The station locations are noted in Figure 17b, along with the tracks of Ophelia in each simulation.

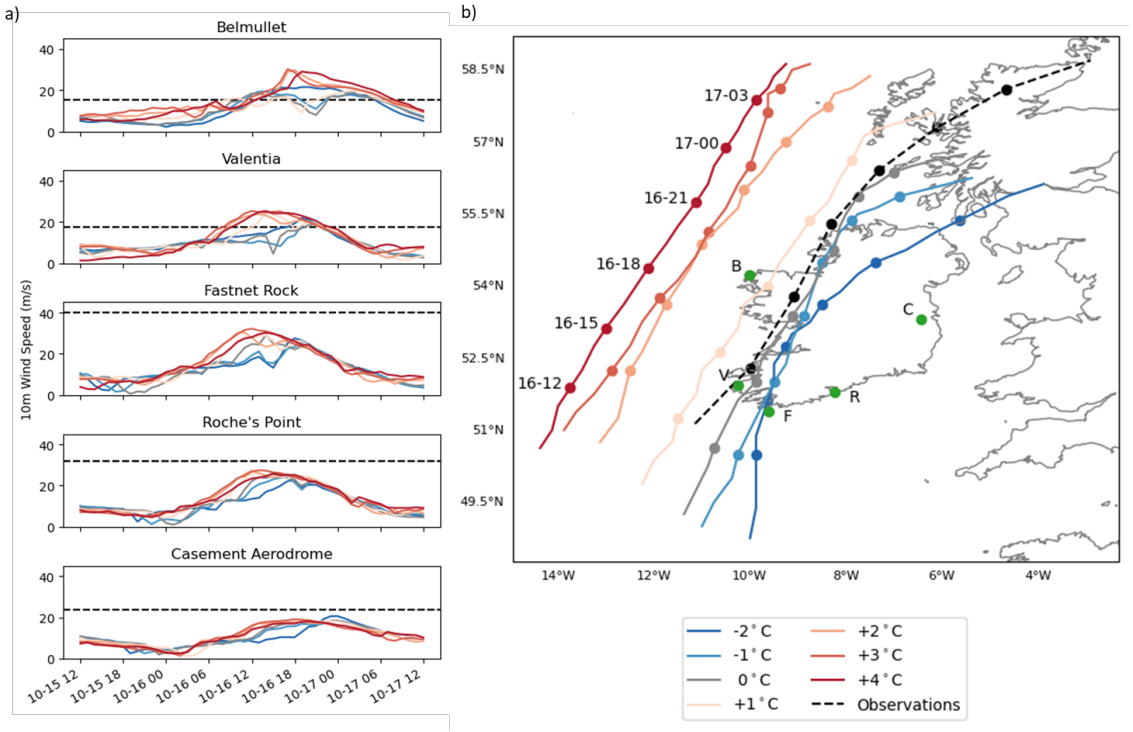

Figure 17: (a) 10m windspeed at five measuring stations around Ireland for each alternate climate scenario, as well as the 10 minute maximum wind speed recorded (b) Locations of the measuring stations (labelled by first letter) are indicated by a green circle. Simulation and observation tracks are plotted between 16 October 09Z and 17 October 06Z. Observations from Met Éireann (2018) and Stewart (2018)

The scenarios with positive temperature forcing have higher winds than the scenarios with negative forcing at nearly every station, the exception being Casement Aerodrome. There the -2°C simulation of Ophelia brings the fastest winds, though the difference is minor; the -2°C has a peak of approximately 20.6 m/s, 2.8 m/s greater than the lowest maximum wind (17.8 m/s in the +2°C scenario). Casement Aerodrome is the station furthest away from the tracks of Ophelia and the furthest inland station, both factors that decrease the expected wind speeds (Kruk et al., 2010). Additionally, the -2°C simulation has Ophelia turning towards it after landfall, decreasing the distance to the station.

Warmer simulations do all have earlier arrival of maximum winds, likely owing to their larger radius. Arrival time is mostly linearly correlated with increased temperature forcing, though the +4°C lags behind the +2°C and +3°C. However this can be explained by its larger distance from land. The Valentia and Fastnet Rock stations both show a sharp dip in wind speeds around 16 October 15Z, which corresponds to the time the center of Ophelia tracked over or close to them, a wind signature reminiscent of a TC-like calm eye. While this lags behind Ophelia's actual landfall time by about 4 hours, this is consistent with the along-track position error seen in Section 4.2.2. We also see that while Valentia and Belmullet have relatively good agreement with the observed 10 minute maximum wind speed for the 0°C simulation, the other stations all underestimate the maximum winds.

The underestimation of observed winds is interesting for Fastnet Rock and Roche's Point especially, which respectively recorded the highest sustained wind speeds overall and the highest sustained wind speeds on land. It calls into question the ability of even the relatively high resolution of RACMO to model the high wind speeds and sharp gradients associated with them in cyclones.

5 Limitations and Future Work

This study examines Hurricane Ophelia as a case study in potential future TC impacts, to determine how its characteristics, ET, and impacts change under alternate climate scenarios, and how well these are modelled.

Despite the improvements in our dynamical models over the last few decades, it is still a challenge to accurately model TCs, even with high-resolution models. We see this in how the ECMWF Operational dataset, which is approximately the same resolution as RACMO, could not adequately simulate Ophelia's intensity, especially in the tropical phase. Pairing this with the conclusion from Majumdar et al. (2023) that even the ECMWF IFS 4 km resolution cannot simulate the strength of TCs indicates that the processes present in the storm are still more complex than covered by the current model physics. The difference in modelling accuracy between the tropical and the extratropical phases may be related to the storm radius increasing and the sharp gradients decreasing as Ophelia underwent ET. However, the examination of the reasons for differing model performance was outside the scope of this study to examine and we leave it for future research.

The analysis datasets we used are advantageous in that they have consistent, global data coverage across space and time (especially in the case of reanalysis datasets), even in areas where the record of observations is spotty or non-existent. The large number of variables available on many different levels of the atmosphere, even ones that are difficult to measure directly make them a very valuable tool. Additionally they reduce the data's sensitivity to outliers by combining many datapoints and creating a best fit, often by method of a nearest-neighbour-type approach.

Unfortunately, because of the global extent of these datasets, their resolution is coarser than that of most regular weather models. While this is not a big problem for large-scale climatological studies, when examining smaller-scale phenomena, such as single TCs, this can be difficult. Also, while the outliers do get smoothed out, long-term biases can creep in, especially in observation-poor areas. Crucially for this study this smoothing also can smooth out extreme gradients such as those found around a TC.

The use of uniform warming (ΔT) over pseudo-global warming (PGW) is to simplify the scenario and provide a clear signal. While the use of a uniform warming scenario is generally fine for RACMO, with a larger domain such as the one used here the question arises if this is physically realistic.

We know from other studies that the polar regions have been warming and will continue to warm up more than the equatorial regions (Manabe and Stouffer, 1980;Serreze et al., 2009). This could counteract some of the strengthening of the jet stream we see in our simulations due to a decrease in meridional temperature gradient (Barnes and Polvani, 2013; Stendel et al., 2021). However, the simplicity and signal clarity the use of uniform warming introduces is determined to be worth it for this first study into the effect of future warming on TCs. Additionally, it provides two strong motivations for a future comparison with Ophelia in a PGW-based scenario: first, to determine if the linear increases in storm intensity and track placement we see are comparable to the results of the more complex PGW scenarios, and second to see if the altered jet stream changes the position of Ophelia's landfall and impacts on Ireland.

We chose to end our analysis of the simulations at 17 Oct 12Z. This is firstly because the portion of the storm we are interested in occurs before and during landfall in Ireland, and by 17 Oct 12Z the storm has passed over the British Isles. While the storm does affect Scandinavia after this time, the wind speeds have greatly decreased and it is dissipating (See Figure 12). Secondly, after this point the storm starts interacting with the boundaries of our regional model (see Figure S4). This effect is more pronounced in the warmer storms, likely because of their larger radius and the greater discrepancy between them and the boundary conditions.

We did not find a cause for the large discrepancies in track and pressure profiles in the RACMO current climate scenarios (Section 4.2.1, though the 200 hPa wind and MSLP were examined as driving factors (not shown). An avenue for future research would be to determine the reason for these discrepancies. One possible path would be to examine the height of the potential vorticity anomaly, as this has been shown to affect the propagation direction (Prater and Evans, 2002).

Following the work of EH2003, we defined the start of ET as the thermal asymmetry increasing over a 10 m threshold. However, as this calculation is based on the height difference between two given layers of the atmosphere. With a warming atmosphere we can expect to see the height difference increase, at which point the value of 10 m would not be the same relative difference as we see now. This provides an avenue of future research, perhaps through method of long climate simulations to examine how ET changes in a warmer world, with for example the empirical

methodologies of EH2003 or the K-clustering of Studholme et al. (2015).

Another extension to this project would be to simulate Ophelia in a different regional model, such as HARMONIE. HARMONIE has several advantages over RACMO: the resolution is higher and the model is non-hydrostatic. A hydrostatic model (such as RACMO) uses the hydrostatic approximation (the assumption that the horizontal scale is much greater than the vertical scale, allowing the vertical acceleration to be negligible) to simplify the equations of motion. This is valid in many large-scale phenomena, but in storms with strong updrafts this fails. This could explain some of the push towards stronger storms we see in RACMO. However, a higher-resolution non-hydrostatic model is more expensive to run. Based on the initial work done in this study, this could nevertheless be a logical next step.

6 Conclusion

The modelling of tropical cyclones continues to be a challenge, but it is a necessary one to take on if we are to understand the threat they may pose to us in a future in which our world has been altered by anthropogenic climate change. We modelled 2017's Hurricane Ophelia as an example of the type of storm we may see in Europe in the future. Examining Ophelia in three analysis datasets (ERA5, ECMWF Operational, and GFS) leads to the conclusion that ECMWF-based models have trouble simulating especially the tropical phase of the storm, even with a high-resolution version of the model. GFS provides a more accurate picture of especially the early intensification of the storm.

Initializing the storm at 24 hour intervals in our regional model RACMO, forced by this GFS data, we find that this case is very sensitive to initial conditions, with large differences in track placement and central pressure between initializations. Selecting the initialization that most closely resembled Ophelia, we applied a uniform temperature change to the initial data (seven simulations, -2 °C to +4 °C with steps of 1 °C), and determined that in warmer climates Ophelia became a larger, more intense storm, which impacted Ireland with higher winds on a wide miss than in the control simulation where it hit directly. In cooler climates, Ophelia remained a weaker storm that tracked closer to mainland Europe,

The extratropical transition of Ophelia is also different under different temperature conditions; in warmer scenarios, Ophelia becomes less asymmetrical and does so later than in cooler scenarios. Ophelia also maintains its warm core nature far longer than in the cooler scenarios. Essentially, in the warmest scenarios Ophelia does not complete ET but remains a hybrid of a tropical and an extratropical storm.

The results of this study should be viewed in the light that this is a simplified case study of one storm and so cannot provide a definitive answer of the impact of future TCs and PTCs on Europe. However, our results are consistent with previous studies on this topic, and this growing body of evidence indicates that there is an increased likelihood of greater impacts in warmer climates. More detailed studies would have to be done of different cases, potentially with PGW scenarios, before more definite conclusions can be drawn.

7 Appendix A

Table 5: Greenhouse gas concentrations in RACMO simulations, as taken from CMIP5-RCP8.5 for October of 2017

Gas	CO_2	CH_4	N_2O	$CFC11$	$CFC12$
Concentration	407.922 ppmv	1.87473 ppmv	329.009 ppbv	210.227 pptv	495.062 pptv

8 Supplemental

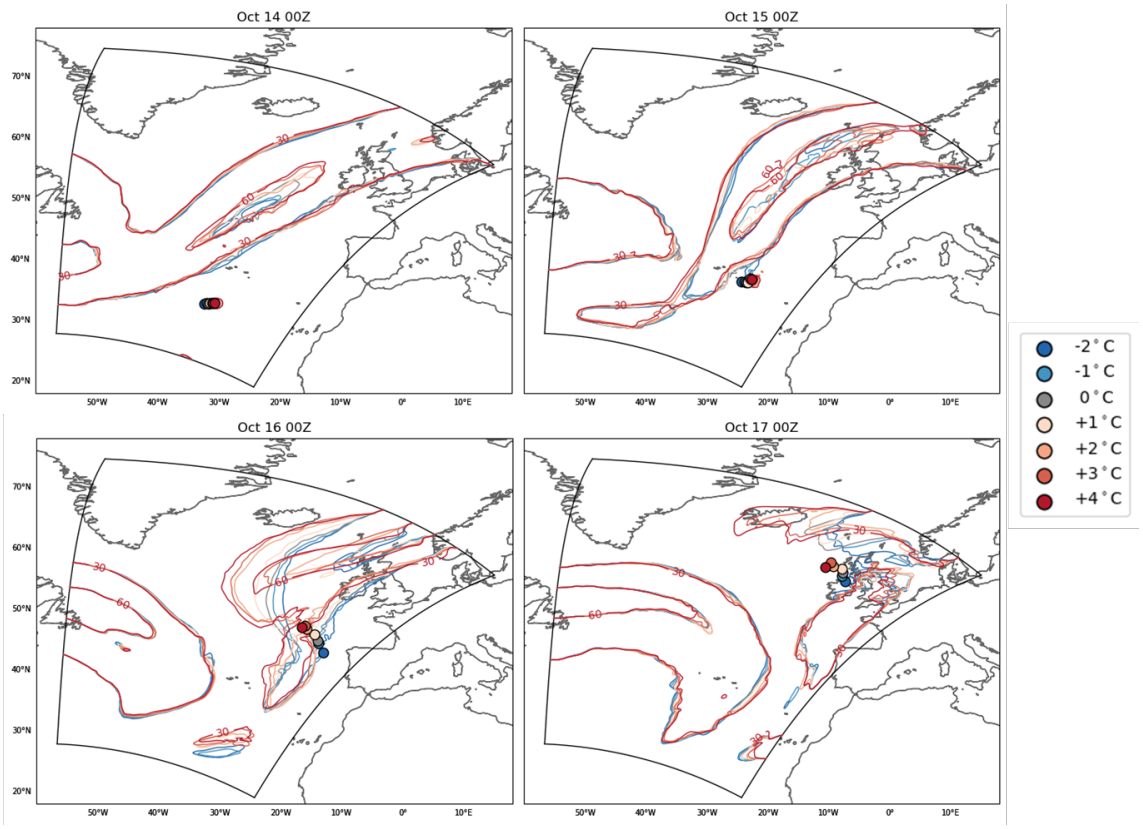

Figure S1: 200 hPa wind speed at 14 - 17 Oct 00Z for each temperature scenarios, 30 m/s contours, with the position of Ophelia at each time plotted as a circle.

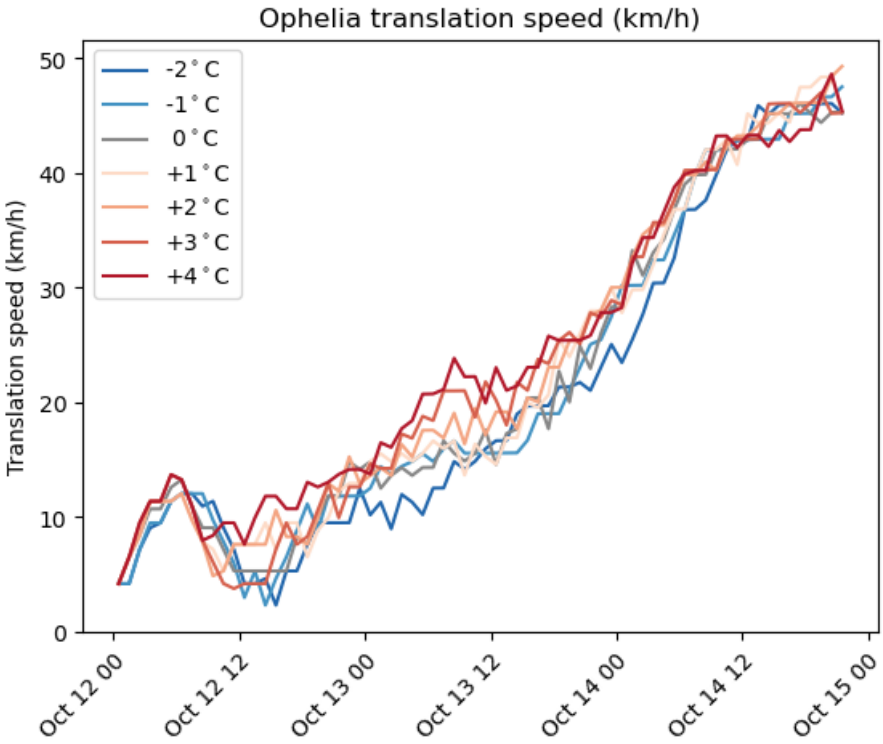

Figure S3: Translation speed of Ophelia in km/h for each scenario for the first 72 hours of the simulations.

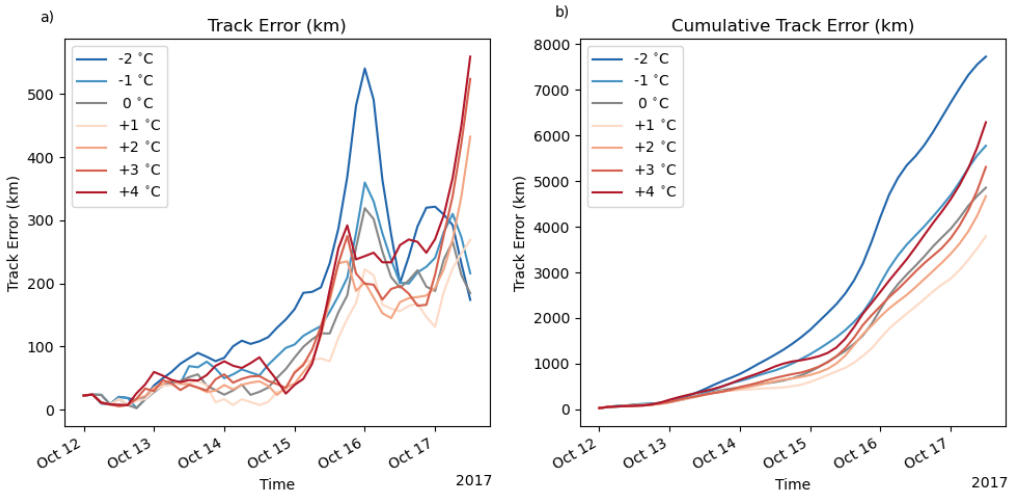

Figure S2: Track error (a) and cumulative track error (b) of downscaled RACMO simulations of Hurricane Ophelia in alternate climates with GFS boundaries, initialized at 24 hour intervals, compared to observations from IBTrACS.

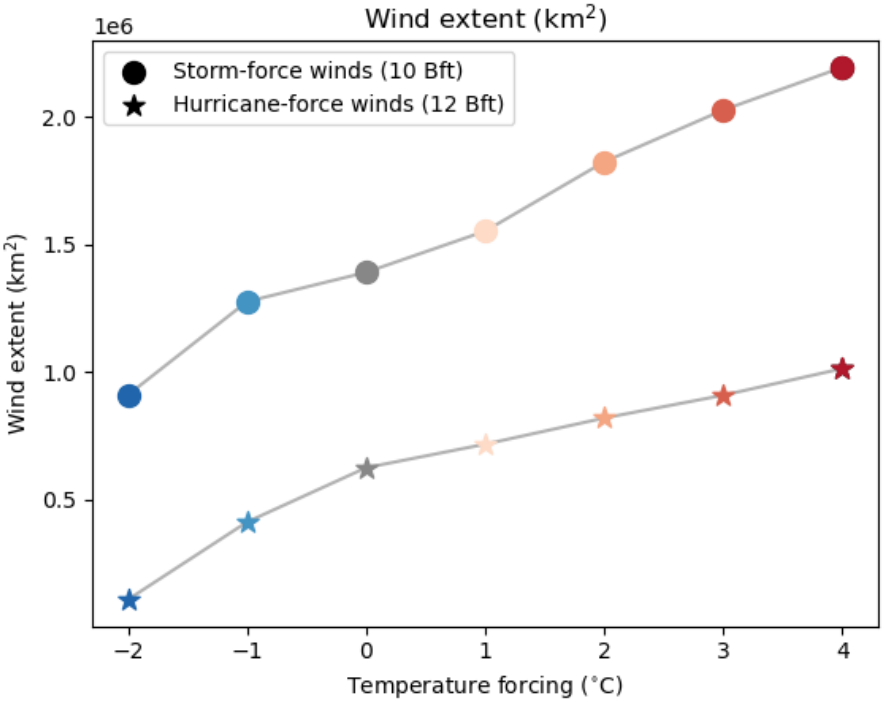

Figure S4: Area extent of storm- and hurricane-force winds (10 and 12 Bft) associated with Ophelia for each of the alternate climate temperature forcings.

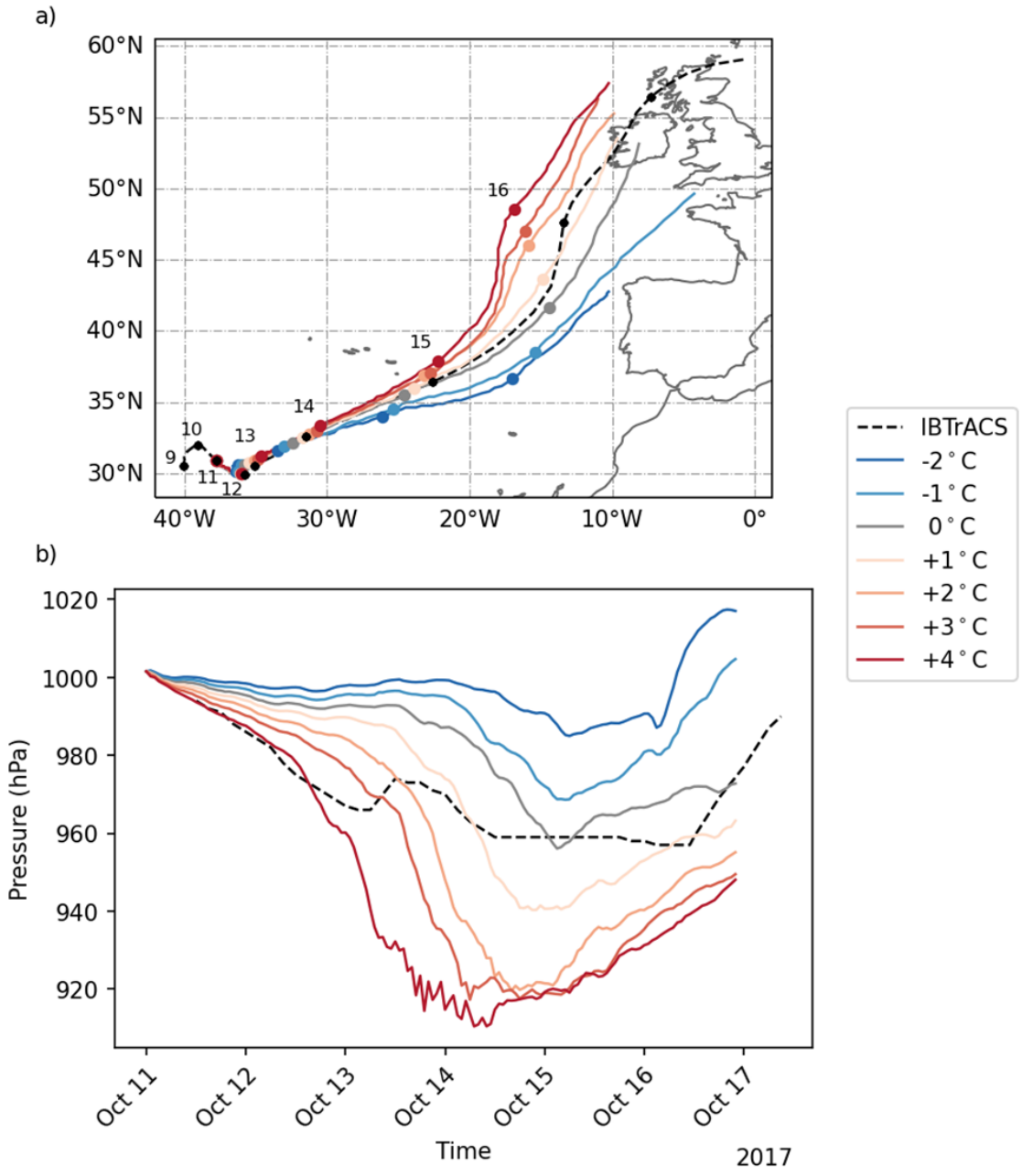

Figure S5: Track (a) and central pressure minimum profiles (b) of Hurricane Ophelia for the alternate climate downscaled RACMO simulations with GFS boundaries, initialized at 00Z 11 October 2017. (a) Circles plotted at 00Z of the date indicated.

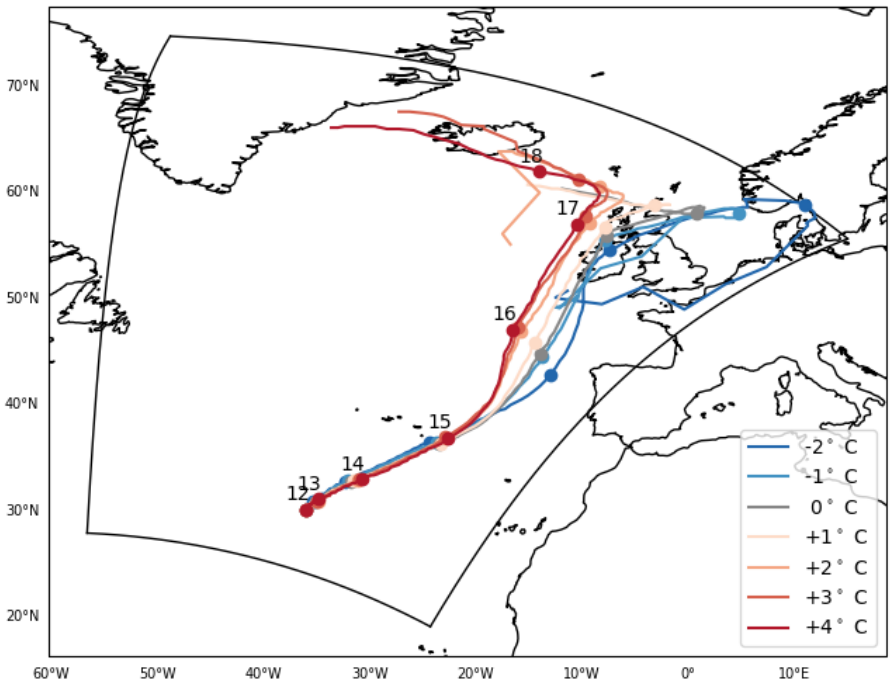

Figure S6: Tracks for Ophelia in each of the alternate climate scenarios for the extended simulation length (until the end of 18 October) laid over the bounds of the regional simulation.

9 References

References

Baatsen, M., Haarsma, R. J., Van Delden, A. J., & De Vries, H. (2015). Severe Autumn storms in future Western Europe with a warmer Atlantic Ocean. *Climate Dynamics*, *45*(3-4), 949–964. https://doi.org/10.1007/s00382-014-2329-8

Barnes, E. A., & Polvani, L. (2013). Response of the Midlatitude Jets, and of Their Variability, to Increased Greenhouse Gases in the CMIP5 Models. *Journal of Climate*, *26*(18), 7117–7135. https://doi.org/10.1175/JCLI-D-12-00536.1

Bolton, D. (1980). The Computation of Equivalent Potential Temperature. *Monthly Weather Review*, *108*(7), 1046–1053. https://doi.org/10.1175/1520-0493(1980)108⟨1046:TCOEPT⟩2.0.CO;2

Camargo, S. J., & Wing, A. A. (2016). Tropical cyclones in climate models. *WIREs Climate Change*, *7*(2), 211–237. https://doi.org/10.1002/wcc.373

Chavas, D. R., Reed, K. A., & Knaff, J. A. (2017). Physical understanding of the tropical cyclone wind-pressure relationship. *Nature Communications*, *8*(1), 1360. https://doi.org/10.1038/s41467-017-01546-9

Colman, R. A., & McAvaney, B. J. (1997). A study of general circulation model climate feedbacks determined from perturbed sea surface temperature experiments. *Journal of Geophysical Research: Atmospheres*, *102*(D16), 19383–19402. https://doi.org/10.1029/97JD00206

Courtney, J., & Knaff, J. (2009). Adapting the Knaff and Zehr wind-pressure relationship for operational use in Tropical Cyclone Warning Centres. *Australian Meteorological and Oceanographic Journal*, *58*, 167–179. https://doi.org/10.22499/2.5803.002

Daloz, A. S., & Camargo, S. J. (2018). Is the poleward migration of tropical cyclone maximum intensity associated with a poleward migration of tropical cyclone genesis? *Climate Dynamics*, *50*(1), 705–715. https://doi.org/10.1007/s00382-017-3636-7

Davis, C. A. (2018). Resolving Tropical Cyclone Intensity in Models. *Geophysical Research Letters*, *45*(4), 2082–2087. https://doi.org/10.1002/2017GL076966

Dekker, M. M., Haarsma, R. J., de Vries, H., Baatsen, M., & van Delden, A. J. (2018). Characteristics and development of European cyclones with tropical origin in reanalysis data. *Climate Dynamics*, *50*(1), 445–455. https://doi.org/10.1007/s00382-017-3619-8

DeMaria, M., Sampson, C. R., Knaff, J. A., & Musgrave, K. D. (2014). Is Tropical Cyclone Intensity Guidance Improving? *Bulletin of the American Meteorological Society*, *95*(3), 387–398. https://doi.org/10.1175/BAMS-D-12-00240.1

Dullaart, J. M. C., de Vries, H., Bloemendaal, N., Aerts, J. C. J. H., & Muis, S. (in press). Improving our understanding of future tropical cyclone intensities in the caribbean using a high-resolution regional climate model.

ECMWF. (2017). Ifs documentation cy43r3 - part i : Observations. https://doi.org/10.21957/7z1cf0t3c

Evans, J. L., & Hart, R. E. (2003). Objective Indicators of the Life Cycle Evolution of Extratropical Transition for Atlantic Tropical Cyclones. *Monthly Weather Review*, *131*(5), 909–925. https://doi.org/10.1175/1520-0493(2003)131⟨0909:OIOTLC⟩2.0.CO;2

Grønas, S. (1995). The seclusion intensification of the New Year's day storm 1992. *Tellus A: Dynamic Meteorology and Oceanography*, *47A*.

Haarsma, R. J., Hazeleger, W., Severijns, C., De Vries, H., Sterl, A., Bintanja, R., Van Oldenborgh, G. J., & Van Den Brink, H. W. (2013). More hurricanes to hit western Europe due to global warming: MORE HURRICANES HIT EUROPE IN FUTURE. *Geophysical Research Letters*, *40*(9), 1783–1788. https://doi.org/10.1002/grl.50360

Hart, R. E. (2003). A Cyclone Phase Space Derived from Thermal Wind and Thermal Asymmetry. *Monthly Weather Review*, *131*(4), 585–616. https://doi.org/10.1175/1520-0493(2003)131⟨0585:ACPSDF⟩2.0.CO;2

Hart, R. E. (2006). Synoptic Composites of the Extratropical Transition Life Cycle of North Atlantic Tropical Cyclones: Factors Determining Posttransition Evolution in: Monthly Weather Review Volume 134 Issue 2 (2006).

Hart, R. E., & Evans, J. L. (2001). A Climatology of the Extratropical Transition of Atlantic Tropical Cyclones. *Journal of Climate*, *14*(4), 546–564. https://doi.org/10.1175/1520-0442(2001)014⟨0546:ACOTET⟩2.0.CO;2

Held, I. M., & Soden, B. J. (2000). Water Vapor Feedback and Global Warming. *Annual Review of Energy and the Environment*, *25*(1), 441–475. https://doi.org/10.1146/annurev.energy.25.1.441

Held, I. M., & Soden, B. J. (2006). Robust Responses of the Hydrological Cycle to Global Warming. *Journal of Climate*, *19*(21), 5686–5699. https://doi.org/10.1175/JCLI3990.1

Hersbach, H., Bell, B., Berrisford, P., Hirahara, S., Horányi, A., Muñoz-Sabater, J., Nicolas, J., Peubey, C., Radu, R., Schepers, D., Simmons, A., Soci, C., Abdalla, S., Abellan, X., Balsamo, G., Bechtold, P., Biavati, G., Bidlot, J., Bonavita, M., ... Thépaut, J.-N. (2020). The ERA5 global reanalysis. *Quarterly Journal of the Royal Meteorological Society*, *146*(730), 1999–2049. https://doi.org/10.1002/qj.3803

Ito, K., Kuroda, T., Saito, K., & Wada, A. (2015). Forecasting a Large Number of Tropical Cyclone Intensities around Japan Using a High-Resolution Atmosphere–Ocean Coupled Model. *Weather and Forecasting*, *30*(3), 793–808. https://doi.org/10.1175/WAF-D-14-00034.1

Jones, E., Parfitt, R., & Wing, A. A. (2024). Development of frontal boundaries during the extratropical transition of tropical cyclones. *Quarterly Journal of the Royal Meteorological Society*, *n/a*(n/a). https://doi.org/https://doi.org/10.1002/qj.4633

Jones, S. C., Harr, P. A., Abraham, J., Bosart, L. F., Bowyer, P. J., Evans, J. L., Hanley, D. E., Hanstrum, B. N., Hart, R. E., Lalaurette, F., Sinclair, M. R., Smith, R. K., & Thorncroft, C. (2003). The Extratropical Transition of Tropical Cyclones: Forecast Challenges, Current Understanding, and Future Directions. *Weather and Forecasting*, *18*(6), 1052–1092. https://doi.org/10.1175/1520-0434(2003)018⟨1052:TETOTC⟩2.0.CO;2

Kitabatake, N. (2011). Climatology of Extratropical Transition of Tropical Cyclones in the Western North Pacific Defined by Using Cyclone Phase Space. *Journal of the Meteorological Society of Japan. Ser. II*, *89*(4), 309–325. https://doi.org/10.2151/jmsj.2011-402

Knapp, K. R., Kruk, M. C., Levinson, D. H., Diamond, H. J., & Neumann, C. J. (2010). The international best track archive for climate stewardship (ibtracs): Unifying tropical cyclone data. *Bulletin of the American Meteorological Society*, *91*(3), 363–376. https://doi.org/10.1175/2009BAMS2755.1

Knutson, T. R., McBride, J. L., Chan, J., Emanuel, K., Holland, G., Landsea, C., Held, I., Kossin, J. P., Srivastava, A. K., & Sugi, M. (2010). Tropical cyclones and climate change. *Nature Geoscience*, *3*(3), 157–163. https://doi.org/10.1038/ngeo779

Kossin, J. P., Emanuel, K. A., & Vecchi, G. A. (2014). The poleward migration of the location of tropical cyclone maximum intensity. *Nature*, *509*(7500), 349–352. https://doi.org/10.1038/nature13278

Kruk, M. C., Gibney, E. J., Levinson, D. H., & Squires, M. (2010). A Climatology of Inland Winds from Tropical Cyclones for the Eastern United States. *Journal of Applied Meteorology and Climatology*, *49*(7), 1538–1547. https://doi.org/10.1175/2010JAMC2389.1

Liu, M., Vecchi, G. A., Smith, J. A., & Murakami, H. (2017). The Present-Day Simulation and Twenty-First-Century Projection of the Climatology of Extratropical Transition in the North Atlantic. *Journal of Climate*, *30*(8), 2739–2756. https://doi.org/10.1175/JCLI-D-16-0352.1

Luu, L. N., van Meijgaard, E., Philip, S. Y., Kew, S. F., de Baar, J. H. S., & Stepek, A. (2023). Impact of Surface Roughness Changes on Surface Wind Speed Over Western Europe: A Study With the Regional Climate Model RACMO. *Journal of Geophysical Research: Atmospheres*, *128*(12), e2022JD038426. https://doi.org/10.1029/2022JD038426

Majumdar, S. J., Magnusson, L., Bechtold, P., Bidlot, J. R., & Doyle, J. D. (2023). Advanced Tropical Cyclone Prediction Using the Experimental Global ECMWF and Operational Regional COAMPS-TC Systems. *Monthly Weather Review*, *151*(8), 2029–2048. https://doi.org/10.1175/MWR-D-22-0236.1

Manabe, S., & Stouffer, R. J. (1980). Sensitivity of a global climate model to an increase of co2 concentration in the atmosphere. *Journal of Geophysical Research: Oceans*, *85*(C10), 5529–5554. https://doi.org/https://doi.org/10.1029/JC085iC10p05529

Mendelsohn, R., Emanuel, K., Chonabayashi, S., & Bakkensen, L. (2012). The impact of climate change on global tropical cyclone damage. *Nature Climate Change*, *2*(3), 205–209. https://doi.org/10.1038/nclimate1357

Met Éireann. (2018). *An Analysis of Storm Ophelia which struck Ireland on the 16th October 2017* (tech. rep.). Met Éireann.

National Centers For Environmental Prediction/National Weather Service/NOAA/U.S. Department Of Commerce. (2015). NCEP GFS 0.25 Degree Global Forecast Grids Historical Archive. https://doi.org/10.5065/D65D8PWK

National Hurricane Center Forecast Verification. (n.d).

NDFEM. (2019). *Review Report on Severe Weather Events 2017 - 2018* (tech. rep.).

Noël, B., van de Berg, W. J., van Meijgaard, E., Kuipers Munneke, P., van de Wal, R. S. W., & van den Broeke, M. R. (2015). Evaluation of the updated regional climate model RACMO2.3: Summer snowfall impact on the Greenland Ice Sheet. *The Cryosphere*, *9*(5), 1831–1844. https://doi.org/10.5194/tc-9-1831-2015

Pasch, R. J., Blake, E. S., Cobb III, H. D., & Roberts, D. P. (2006). Tropical Cyclone Report.

Pielke, R. A., Gratz, J., Landsea, C. W., Collins, D., Saunders, M. A., & Musulin, R. (2008). Normalized Hurricane Damage in the United States: 1900–2005. *Natural Hazards Review*, *9*(1), 29–42. https://doi.org/10.1061/(ASCE)1527-6988(2008)9:1(29)

Prater, B. E., & Evans, J. L. (2002). Sensitivity of modeled tropical cyclone track and structure of hurricane Irene (1999) to the convective parameterization scheme. *Meteorology and Atmospheric Physics*, *80*(1), 103–115. https://doi.org/10.1007/s007030200018

Quitián-Hernández, L., González-Alemán, J. J., Santos-Muñoz, D., Fernández-González, S., Valero, F., & Martín, M. L. (2020). Subtropical Cyclone Formation via Warm Seclusion Development: The Importance of Surface Fluxes. *Journal of Geophysical Research: Atmospheres*, *125*(8), e2019JD031526. https://doi.org/10.1029/2019JD031526

Radu, R., Toumi, R., & Phau, J. (2014). Influence of atmospheric and sea surface temperature on the size of hurricane Catarina. *Quarterly Journal of the Royal Meteorological Society*, *140*(682), 1778–1784. https://doi.org/10.1002/qj.2232

Rantanen, M., Räisänen, J., Sinclair, V. A., & Lento, J. (2020). The extratropical transition of Hurricane Ophelia (2017) as diagnosed with a generalized omega equation and vorticity equation. *Tellus A: Dynamic Meteorology and Oceanography*, *72*(1), 1721215. https://doi.org/10.1080/16000870.2020.1721215

Saarinen, S. (2004, May). Ifs documentation cy33r1 - part i: Observation processing [¡p¿ ODB User Guide¡/p¿]. ECMWF. https://doi.org/10.21957/bj0w7aul

San-Miguel-Ayanz, J., Oom, D., Artes, T., Viegas, D., Fernandes, P., Faivre, N., Freire, S., Moore, P., Rego, F., & Castellnou, M. (2020, December). Forest fires in Portugal in 2017.

Serreze, M. C., Barrett, A. P., Stroeve, J. C., Kindig, D. N., & Holland, M. M. (2009). The emergence of surface-based Arctic amplification. *The Cryosphere*, *3*(1), 11–19. https://doi.org/10.5194/tc-3-11-2009

Shapiro, M. A., & Keyser, D. (1990). Fronts, Jet Streams and the Tropopause. In C. W. Newton & E. O. Holopainen (Eds.), *Extratropical Cyclones: The Erik Palmén Memorial Volume* (pp. 167–191). American Meteorological Society. https://doi.org/10.1007/978-1-944970-33-8_10

Simpson, R. H., & Saffir, H. (1974). The Hurricane Disaster—Potential Scale. *Weatherwise*, *27*(4), 169–186. https://doi.org/10.1080/00431672.1974.9931702

Smith, A. B. (2023). U.S. Billion-dollar Weather and Climate Disasters, 1980 - present (NCEI Accession 0209268). https://doi.org/10.25921/STKW-7W73

Srinivas, C. V., Mohan, G. M., Naidu, C. V., Baskaran, R., & Venkatraman, B. (2016). Impact of air-sea coupling on the simulation of tropical cyclones in the North Indian Ocean using a simple 3-D ocean model coupled to ARW. *Journal of Geophysical Research: Atmospheres*, *121*(16), 9400–9421. https://doi.org/10.1002/2015JD024431

Stendel, M., Francis, J., White, R., Williams, P. D., & Woollings, T. (2021). The jet stream and climate change. In *Climate Change* (pp. 327–357). Elsevier. https://doi.org/10.1016/B978-0-12-821575-3.00015-3

Stewart, S. R. (2018). *Tropical Cyclone Report: Hurricane Ophelia, 9–15 October 2017* (tech. rep.). National Hurricane Center.

Studholme, J., Fedorov, A. V., Gulev, S. K., Emanuel, K., & Hodges, K. (2022). Poleward expansion of tropical cyclone latitudes in warming climates. *Nature Geoscience*, *15*(1), 14–28. https://doi.org/10.1038/s41561-021-00859-1

Studholme, J., Hodges, K. I., & Brierley, C. M. (2015). Objective determination of the extratropical transition of tropical cyclones in the northern hemisphere. *Tellus A: Dynamic Meteorology and Oceanography*. https://doi.org/10.3402/tellusa.v67.24474

Taylor, K. E., Stouffer, R. J., & Meehl, G. A. (2012). An overview of cmip5 and the experiment design. *Bulletin of the American Meteorological Society*, *93*(4), 485–498. https://doi.org/10.1175/BAMS-D-11-00094.1

Thorncroft, C., & Jones, S. C. (2000). The Extratropical Transitions of Hurricanes Felix and Iris in 1995. *Monthly Weather Review*, *128*(4), 947–972. https://doi.org/10.1175/1520-0493(2000)128⟨0947:TETOHF⟩2.0.CO;2

van Meijgaard, E., van Ulft, L., Lenderink, G., de Roode, S., Wipfler, E., Boers, R., & van Timmermans, R. (2012a). *Refinement and application of a regional atmospheric model for climate scenario calculations of western europe*. KVR.

van Meijgaard, E., van Ulft, L. H., Lenderink, G., de Roode, S. R., Wipfler, E. L., Boers, R., & van Timmermans, R. M. A. (2012b). *Refinement and application of a regional atmospheric model for climate scenario calculations of Western Europe* (tech. rep.). KVR.

Xu, Z., & Yang, Z.-L. (2012). An improved dynamical downscaling method with gcm bias corrections and its validation with 30 years of climate simulations. *Journal of Climate*, *25*(18), 6271–6286. https://doi.org/10.1175/JCLI-D-12-00005.1